

# Biogeographic pattern of microbial communities inhabiting terrestrial mud volcanoes across the Eurasian continent

Tzu-Hsuan Tu<sup>1,2,3</sup>, Li-Ling Chen<sup>2</sup>, Yi-Ping Chiu<sup>3</sup>, Li-Hung Lin<sup>3,4</sup>, Li-Wei Wu<sup>5</sup>, Francesco Italiano<sup>6</sup>, J. Bruce H. Shyu<sup>3</sup>, Seyed Naser Raisossadat<sup>7,8</sup>, and Pei-Ling Wang<sup>2,4\*</sup>

<sup>1</sup>Department of Oceanography, National Sun Yat-sen University, Kaohsiung, Taiwan

<sup>2</sup>Institute of Oceanography, National Taiwan University, Taipei, Taiwan

<sup>3</sup>Department of Geosciences, National Taiwan University, Taipei, Taiwan

<sup>4</sup>Research Center for Future Earth, National Taiwan University, Taipei, Taiwan

<sup>5</sup>Department of Life Science, Tunghai University, Taichung, Taiwan

<sup>6</sup>National Institute of Geophysics and Volcanology, Palermo, Italy

<sup>7</sup>Department of Geology, University of Birjand, Birjand, Iran

<sup>8</sup>Earth Science Research Group, University of Birjand, Birjand, Iran

Correspondence to: Pei-Ling Wang (plwang@ntu.edu.tw)

**Abstract.** Terrestrial mud volcanoes (MVs) represent the surface expression of conduits tapping fluid and gas reservoirs in the deep subsurface. Such plumbing channels provide a direct, effective means to extract deep microbial communities fueled by geologically produced gases and fluids. The drivers accounting for the diversities and compositions of these MV microbial communities distributed over a wide geographic range remain elusive. This study characterized the variation of microbial communities in 15 terrestrial MVs across a distance of ~10,000 km of the Eurasian continent to test the validity of distance control and physiochemical factors in explaining biogeographic patterns. Our analyses yielded diverse community compositions with a total of 28,928 amplicon sequence variants (ASVs) taxonomically assigned to 73 phyla. Although no true cosmopolitan member was found, ~85% of ASVs were confined within a single MV. Community variance between MVs appeared to be higher and more stochastically controlled than within MVs, generating a slope of distance–decay relationship exceeding those for marine seeps and MVs, and seawater columns. For comparison, physiochemical parameters explained 12% of community variance, with chloride concentration being the most influential factor. Overall, the apparent lack of fluid exchange renders terrestrial MVs a patchy habitat, with microbiomes diverging stochastically with distance and consisting dispersal-limited colonists that are highly adapted to the local environmental context.

## 1 Introduction

Microbial biogeography describes the distribution of microbial taxa over space and time, providing insights into the fundamental processes generating and governing diversity (Lomolino et al., 2006). Four nonexclusive processes—selection, drift, dispersal, and mutation—have been proposed to account for various microbial biogeographical patterns (Hanson et al., 2012). The “selection” process is generally regarded as deterministic and involves nonrandom, niche-based mechanisms,

Style Definition: Unresolved Mention

Deleted: Stochastic process determines the spatial variations in

Deleted: community

Formatted: English (US)

Formatted: English (US)

Formatted: English (US)

Formatted: English (US)

Deleted: diversity

Deleted: composition

Deleted: of

Deleted: community

Deleted: geographic locations was

Deleted: sites

Deleted: and specific geochemical parameters were correlated

Deleted: specific taxa.

Deleted: microbiome comprising specific

Deleted: and restricted in terms of dispersal capability

Formatted: English (US)

Formatted: Font color: Black, English (UK)

Deleted: , including

Deleted: ,

Formatted: Font color: Black, English (UK)

Deleted: intrinsically hypothesizes that microbial dispersal is so effective and rapid that the effects of evolutionary and ecological events in accordance with the traits, niche preference, and biological interactions are erased.

including environmental filtering (e.g., pH, temperature, salinity, and geochemical or redox variations) and various biological interactions (e.g., competition, mutualisms, predation, and tradeoffs) (Ning et al., 2019). Therefore, the distribution pattern of microbial diversity is controlled by the response of community members to environmental parameters (Comte et al., 2016; Power et al., 2018). Such selection factors could have led to the establishment of a variety of core microbiomes inhabiting distinct environments, such as soil, sediment, aquatic, and vent ecosystems (Orcutt et al., 2011; Ruff et al., 2015) or organized spatially as in a gradient and, thus, autocorrelated (Hanson et al., 2012; Ranjard et al., 2013). The “drift” process is caused by chance events (e.g., differences of taxa associated with birth and death events), differentiating microbial composition over space in neutral theory (Slatkin, 1993; Condit et al., 2002). Microbial dispersal is defined as the physical movement of cells between two locations and successful establishment at the receiving location (Hanson et al., 2012). Due to the dispersal limitation, chance events at one location would influence nearby compositions. Therefore, the interaction between drift and dispersal limitation would generate a distance–decay relationship (DDR) (Hutchison and Templeton, 1999) in which the community dissimilarity increases with distance. Finally, gene duplications, mutations, and other processes produce new genes and alleles that reshape the DDR by increasing local genetic diversity across all locations. Although these latter three processes generate community diversity patterns indistinguishable from random chance alone or are considered a stochastic consequence (Ning et al., 2019), they are also non-exclusive and interact with deterministic processes. Dissecting the contribution of individual processes and governing factors remains a challenging issue (Hanson et al., 2012).

Mud volcanoes (MVs) represent a unique ecosystem for investigating microbial biogeographic patterns when compared with aquatic, soil, and sediment ecosystems on or near the land surface or seafloor. This uniqueness stems from the fact that the MV’s genesis is tightly linked with the plumbing of fluids and sediments from deep reservoirs through fracture networks often extending to a depth of several kilometers (Mazzini and Etiope, 2017). Because advection dominates over diffusion for fluid transport, relatively rapid migration can occur with minimal alterations of geochemical characteristics and even microbial communities of fluids/muds emanating from a mud cone or pool (Dimitrov, 2002; Chen et al., 2020). Therefore, MVs provide a direct, effective means to recover deep microbial communities. Meanwhile, the export of reducing compounds and rapid deposition of sediments enable MV sediments to be highly reduced and confined to a limited spatial extent (from tens of cms to kilometers) (Chang et al., 2012; Cheng et al., 2012; Mazzini and Etiope, 2017). Such physico-chemical characteristics generate localized, strong redox gradients and host abundant microorganisms with identities distinct from adjacent environments or overlying seawater (Wang et al., 2014; Lin et al., 2018), rendering MVs globally distributed, unique biological hotspots fueled by geologically produced gases and fluids. A recent survey has demonstrated the predominance of few cosmopolitan taxa with a physiological preference for methane or hydrocarbons in marine MVs (Ruff et al., 2015). This line of evidence, combined with the observed DDR, suggests that both dispersal and selection exert a profound influence on shaping community compositions and structures. In contrast to the aid of dispersal through seawater circulation in marine counterparts, terrestrial MVs are even more limitedly connected between each other. For a geographic scale larger than tens of kilometers, dispersal through groundwater transport would be essentially absent. This limitation, combined with enormous oxidative power driven by atmospheric oxygen (Lin et al., 2018) renders the terrestrial MVs ideal for investigating whether any biogeographic

- Formatted: Font color: Black, English (UK)
- Formatted: Font color: Black, English (UK)
- Deleted: spatially
- Formatted: Font color: Black, English (UK)
- Deleted: such as stochastic
- Deleted: among
- Deleted: in
- Deleted: ,
- Deleted: , and migration
- Formatted: Font color: Black, English (UK)
- Formatted: English (US)
- Formatted: Font color: Black, English (UK)
- Deleted: microbial biogeographic
- Deleted: undoubtedly controlled by the evolutionary
- Deleted: ecological interplay of these four
- Deleted: , dissecting
- Deleted: exact
- Deleted: the
- Deleted: surfaces
- Deleted: the
- Deleted: is because MVs’
- Formatted: Font color: Black, English (UK)
- Formatted: Font color: Black, English (UK)
- Formatted: Font color: Black, English (UK)
- Deleted: enables
- Deleted: cm
- Formatted: English (UK)
- Formatted: English (UK)
- Deleted: )
- Deleted: -
- Deleted: Ruff
- Formatted: Font color: Black, English (UK)
- Deleted: 2015
- Formatted: Font color: Black, English (UK)
- Formatted: Font color: Black, English (UK)
- Deleted: distributed globally
- Formatted: Font color: Black, English (UK)
- Deleted: the

110 pattern imposed by geographic isolation and environmental contexts emerges. In addition to various spatial scales, environmental and redox contexts vary substantially along a vertical scale. The variance of beta diversity and its controlling mechanism on both spatial and vertical scales remains poorly constrained.

Deleted: exact

This study aims to determine prokaryotic community compositions and structures associated with terrestrial MVs and to constrain the underlying mechanisms by examining the control of deterministic and stochastic processes on community variations over a spatial scale (up to ~ 10,000 km) across the Eurasian continent and a vertical scale (up to ~ 1.5 m) over a redox transition. Community compositions based on 16S rRNA gene sequences and metadata for cored sediments from 15

Deleted: accounting for such variance

Deleted: of ten-thousand kilometers

115 MVs were synthesized and analyzed to assess the control of qualitative stochasticity on community variations at different spatial and vertical scales using various statistical approaches and ecological metrics. Moreover, while cosmopolitan members with significant dispersal capability and specific colonists highly adapted to local environmental contexts were identified, distribution patterns of members potentially possessing sulfur or methane metabolisms were also revealed. These results were compared with marine data to draw the framework and characteristics shared between terrestrial and marine MV ecosystems.

Deleted: distributed across the Eurasian continent

Deleted: analyzed and

Deleted: address whether

Deleted: are controlled by dispersal

Deleted: /or environmental selection.

Deleted: community

Deleted: .

120 This work represents the most extensive microbial ecology study to date on terrestrial MVs at a continental scale.

## 2 Materials and Methods

Formatted: English (US)

### 2.1 Sampled MVs and data source

125 Muddy fluids from bubbling pools and sediment cores from the adjacent mud platform were retrieved from MVs across the Eurasian continent during 2011 to 2013 (Fig. 1; Table S1) for geochemical (n=9) and molecular analyses (n=13). Detailed sample collection, processing, and preservation are described in the supplementary information. Data obtained in this study were merged with companion geochemical data for 4 MVs in Italy (AR01, COM01, PA01, and PA02; Chiu, 2015), and geochemical and molecular data for 2 MVs in Taiwan (LGH03 and SYNH02; Tu et al., 2017; Lin et al., 2018) to generate a total of 136 sample sets for 16 cores from 15 MVs.

Deleted: Sampling sites

Formatted: English (US)

Deleted: procedures

Formatted: English (US)

Deleted: a total of 16

Deleted: 15

Deleted: 2017

Deleted: TableS1

Deleted: .

Deleted: were

### 2.2 Geochemical analyses

Formatted: English (US)

130 Concentrations of methane were analyzed using a 6890N gas chromatograph (GC; Agilent Technologies, USA). Carbon isotope compositions of methane were measured with a MAT253 isotope ratio mass spectrometer connected to a GC Isolink (Thermo Fisher Scientific, USA). Chloride and sulfate concentrations in porewater were analyzed using an ICS-3000 ion chromatograph (Thermo Fisher Scientific, USA). Concentrations of particulate total organic carbon (TOC), total inorganic

Deleted: and dissolved inorganic carbon (DIC)

Deleted: Santa Clara, CA,

Deleted: and DIC

Deleted: using

Deleted: (IRMS)

Deleted: with

Deleted: Waltham, MA,

Deleted: Waltham, MA,

160 carbon (TIC), total nitrogen (TN), and total sulfur (TS) were determined by an elemental analyzer (MICROcube, Elementar, Germany). Detailed methods for these analyses are described in the supplementary information.

**Deleted:** were

### 2.3 Microbial community analyses

Crude DNA for 16S rRNA gene analyses was extracted from fluids/sediments using a PowerSoil DNA Isolation Kit (Qiagen, Germany). Bubbling fluids (if available) and sediments distributed across geochemical transition were selected for DNA extraction. These samples are representative of communities inhabiting the subsurface source region (for bubbling fluids) or subject to the redox gradient developed after the sediment deposition (cored sediments in the adjacent mud platform). DNA extracts were obtained and stored at  $-80^{\circ}\text{C}$  for subsequent analyses.

**Formatted:** English (US)

**Deleted:** composition

**Deleted:** the

**Deleted:** Hilden,

**Deleted:** subjected

**Deleted:** A total of 136

Amplicons for 16S rRNA genes were generated from polymerase chain reactions (PCR) using the universal primers targeting both bacterial and archaeal communities, and sequenced on the Illumina platform. Sequences were analyzed using Mothur and QIIME2 (Schloss et al., 2009; Bolyen et al., 2018). Denoised reads were assembled to full sequences, aligned, and taxonomically assigned against the Silva v.132 reference set using Mothur. Detailed schemes for PCR, sequencing, and sequence processing are described in the supplementary information. The obtained sequences were deposited in GenBank with accession number PRJNA560274.

**Deleted:** Sequences of 16S rRNA gene amplicons were analyzed using the...

**Formatted:** Font color: Black, English (UK)

**Deleted:** The obtained sequences were deposited in GenBank with accession number PRJNA560274.

**Deleted:** were

### 2.4 Statistic analyses

175 Detailed methods for statistical analyses are described in the supplementary information.

**Formatted:** English (US)

**Deleted:** Statistics

#### 2.4.1 Microbial community analyses

Sequence data were first rarefied to 9,413 sequences per sample through 100 sequence random re-sampling (without replacement) of the original amplicon sequence variant (ASV) table to account for the difference in sequencing depth for the calculation of alpha diversity indices (Hill, 1973). For the beta diversity calculation, the entire ASV table was used and normalized using the function cumNorm embedded within metagenomeSeq in R (Paulson et al., 2013). The method considers the sum of ASVs and their quantile distribution for each sample by adjusting the sequence number for individual ASVs while keeping the total ASVs the same before and after the normalization. The method does not sacrifice the sample diversity contributed from rare ASVs, thereby providing a better assessment of the community variation across different spatial scales or controlled by localized environmental factors. The dissimilarity matrix between samples was computed using the Bray-Curtis method (Bray and Curtis, 1957; Ranjard et al., 2013) and visualized through the ordination of non-metric multidimensional scaling (NMDS). Among the synthesized 136 samples, 126 samples with concentrations of chloride, sulfate,

**Deleted:** Samples

**Formatted:** English (US)

**Formatted:** English (US)

**Deleted:** variants

**Formatted:** English (US)

**Formatted:** Font color: Black

**Deleted:** ; Chao et al., 1984).

**Formatted:** English (US)

**Deleted:** from the R package metagenomeSeq (Paulson et al., 2013)....

**Formatted:** English (US)

**Formatted:** Font color: Black

**Formatted:** English (US)

**Deleted:** )

205 methane, TN, TS, TIC, and TOC were used for constrained correspondence analysis (CCA), which aims to elucidate the relationship between microbial community compositions and geochemical variables.

Formatted ... [1]  
Deleted: .  
Formatted: English (US)

#### 2.4.2 Habitat similarities

Deleted: Estimation of habitat

210 Habitat similarities were calculated from the Euclidean distances between paired 126 samples with the available concentrations of chloride, sulfate, methane, TN, TS, TIC, and TOC using the following equation (Ranjard et al., 2013):

Deleted: An estimation of habitat  
Formatted: English (US)  
Deleted: was  
Formatted: English (US)  
Deleted: . The transformed dataset was used to evaluate habitat similarity

$$E_d = \left(1 - \frac{Euc_d}{Euc_{max}}\right) \quad (1)$$

Formatted: English (US)  
Deleted: Eq. (1)  
Formatted: English (US)  
Formatted: English (US)

where  $E_d$  is the habitat similarity,  $Euc_d$  is the Euclidean distance, and  $Euc_{max}$  is the maximum distance between MVs.

#### 2.4.3 Distance decay relationships (DDR)

215 To assess the DDR, pairwise community similarities were calculated using the Sørensen-Dice index (Dice, 1945). The pairwise similarity was transformed in a logarithmic scale to enhance the linear fitting (Nekola and White, 1999) using the following equation:

Formatted ... [2]  
Deleted: .  
Formatted: English (US)

$$\log_{10}(S_{com}) = \log_{10}(a) + \beta \log_{10}(D) \quad (2)$$

Deleted: sites in the matrix  
Formatted: English (US)  
Formatted: English (US)  
Deleted: between samples  
Formatted: English (US)

220 where  $S_{com}$  is the pairwise similarity in community composition,  $D$  is the distance between two samples,  $a$  is the intercept, and  $\beta$  is the slope. The distance between samples was aggregated from two categories for samples in separate cores (geographic distance) or within the same cores (vertical distance).

Deleted: -  
Formatted ... [4]  
Deleted: space

#### 2.4.4 Normalized stochasticity ratios (NSTs)

Formatted ... [5]  
Deleted: Eq. (2):

225 NSTs were calculated to assess the stochasticity of community variations within each category of samples using 50% as a threshold for either more stochastic (>50%) or deterministic (<50%) control (Ning et al., 2019). The analysis was conducted using the obtained ASV table by first categorizing all samples into “bubbling fluid”, “surface sediment”, and “within MV sediment”, each representing source communities, source communities subject to minor surface impact, or communities potentially altered by localized geochemical/redox context. The categorization addressed the scenarios whether the variation pattern for source communities with/without minor impact of the surface process (for “bubbling fluid” and “surface sediment”) is dependent on distance separation and whether the variation pattern for localized communities (for “within MV sediment”)

230

Formatted: English (US)  
Formatted ... [6]  
Deleted: .  
Formatted: English (US)  
Formatted: English (US)  
Deleted: geographic and/or vertical  
Formatted ... [7]  
Deleted: .

265 is dependent on a specific environmental context within individual MVs. The NST was calculated using the package NST developed by Ning et al. (2019) based on the Bray–Curtis dissimilarity ( $NST_{bray}$ ), Jaccard distance ( $NST_{jaccard}$ ), and phylogenetic distance (pNST) between pairwise communities within each category of samples, following the recommendation of the developers.

Formatted: English (US)

### 3 Results

#### 270 3.1 Physical and geochemical characteristics

The pairwise distance between samples ranged from 2.5 to 160 cm within cores and 0.005 to 9,924 km between cores (Fig. 1). Geochemical profiles of pore water showed various characteristics related to abiotic and microbial processes. Chloride concentrations varied highly among MVs (ranging between 82 mM at SI02 in Myanmar and 4890 mM at GG01 in Iran) and generally decreased with increasing depth within individual cores (Fig. S1). Sulfate concentrations ranged from below the detectable level at SM22, AK03, GJ01, TA, PA01, PA02, and LGH03 to 288 mM at GG01, with most data clustering between 0.5 and 2 mM. Methane concentrations ranged between 0.006 mM (PA02) and 3.98 mM (SYMH02C4), with most data clustering between 0.2 and 1 mM (Figure S2). The  $\delta^{13}C$  values of methane spanned from -58‰ to -35‰ and exhibited a trend opposite to that of methane concentration. The molar ratios of methane over ethane and propane ( $C1$  (methane) / ( $C2$  (ethane) +  $C3$  (propane))) were variable and ranged from 22 (SI02) to approximately 1200 (AR01 and COM01; Fig. S3). Detailed porewater characteristics are provided in the supplementary information.

Deleted: sites

Deleted: clustered between

Deleted: and

280 Pairwise comparisons between samples within individual cores yielded a habitat similarity ( $Ed$ ) ranging between 0.42 and 1.0 (for data points with a distance of 2.5 to 160 cm in Fig. 2a). These narrow-ranging indices were generally higher than those for samples between cores (for data points with a distance greater than 160 cm in Fig. 2a). Inspection of the data sets, however, demonstrated a contrast pattern between some MVs. For example, the geographic distances between MVs in Italy and Taiwan were the highest among all MV pairs. Habitat similarities between AR01, COM01, and SYNH02, LGH03 were greater than 0.96. In contrast, habitat similarities between GG01 and other MVs were low, even though the geographic distances were short. Overall, habitat similarities were not significantly correlated with vertical distance but horizontal distance ( $P < 0.001$ ) (Fig. 2a).

Deleted: pore-water

Deleted: were described

Deleted: vertical

Deleted:

Deleted: MVs

Deleted: sites

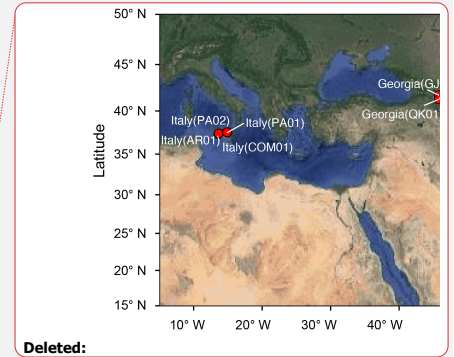
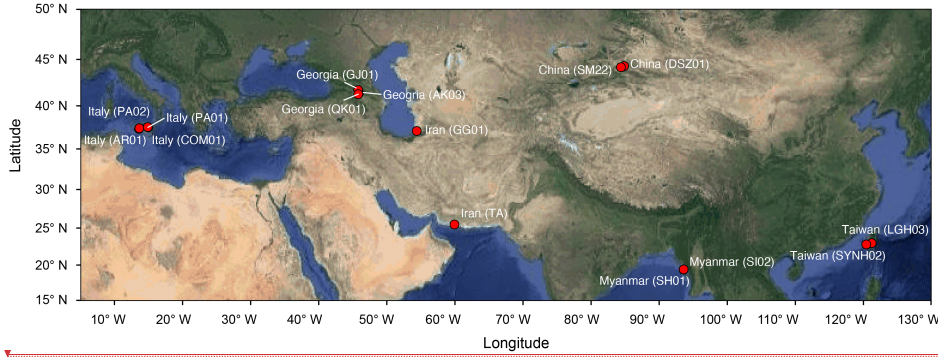
Deleted: sites

Deleted: ,

Deleted: ,

Deleted: , and

Deleted: for



Deleted:

305 **Figure 1:** Map overlay with **analyzed mud volcanos (solid red circles)**. Country names are shown with **MV codes in parentheses**. The map is **modified from Google Maps 2021 using the ggmap package (Kahle and Wickham, 2013) in R**.

Deleted: sampling sites and site

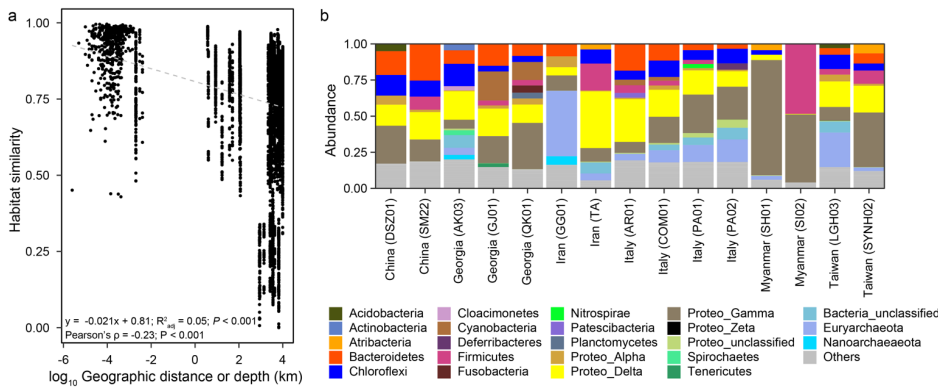
Deleted: across the Eurasian continent. Detailed site information is shown in Table S1.

Deleted: © Google

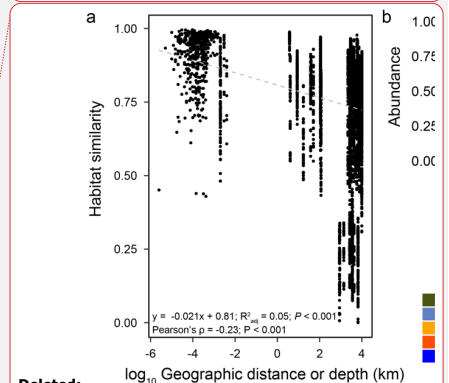
Formatted: English (US)

Deleted: and modified with

Formatted: English (US)



310 **Figure 2:** (a) **Plot of habitat similarity versus geographic distance or depth**. (b) **Abundances of major phyla based on 16S rRNA gene amplicons**. **Raw sequence data for LGH03 and SYNH02 from Tu et al. (2017) and Lin et al. (2018) were incorporated for the analysis and comparison**.



Deleted:

Deleted: Relationship between

Deleted: and

Deleted: revealed by

Formatted: English (US)

### 3.2 Community structures and compositions

325 A total of 24,617 bacterial and 4,311 archaeal ASVs, representing 181 classes (157 bacterial and 24 archaeal) within 73 phyla, were recovered. The observed ASVs for individual samples ranged between 58 and 1,462, with an average value of  $449 \pm 250$  when singletons (presence of one sequence for an ASV at only one depth) were included. The trends of diversity indices were revealed in a similar pattern (Figure S4). The lowest values of alpha diversity indices occurred at SI02 and SH01 in Myanmar, whereas the highest values were found for AR01 in Italy. Diversities at the ASV level were fully captured for individual cores but not sufficiently recovered by taking all cores as a whole (Supplementary information; Figure S5).

330 The dominant phyla and subdivisions of Proteobacteria (>5% of the total reads) included Firmicutes (6.0%), Chloroflexi (7.6%), Euryarchaeota (8.6%), Bacteroidetes (9.5%), Deltaproteobacteria (18.6%), and Gammaproteobacteria (21.4%). The majority of bacterial reads were assigned to the orders Betaproteobacteriales (4.2%), Desulfuromonadales (6.1%), and Desulfobacterales (7.1%). Most sequences belonging to these three orders were related to the families Hydrogenophilaceae (2.9%), Desulfuromonadaceae (3.4%), and Desulfobulbaceae (4.5%), respectively. The two dominant genera, *Thiobacillus* (Hydrogenophilaceae) and *Desulfurivibrio* (Desulfobulbaceae), constituted 2.9% and 3.2% of the total reads, respectively. For comparison, the majority of archaeal reads were assigned to the orders Halobacteriales (2.8%) within Halobacteria and Methanosarcinales (4.3%) within Methanomicrobia. Whereas most sequences assigned to Halobacteria were related to the families Halobacteriaceae (1%) and Haloferacaceae (1.1%), the predominant sequences within Methanomicrobia were affiliated with ANME-2a (3.2%). Among the 28,928 ASVs, five out of the ten most abundant ASVs were affiliated with the genus *Thiobacillus* (0.4–0.7% of the total reads).

340 Of 73 phyla obtained, nine were found in all cores, and the other nine in only one core (Figs. 2b & 3a). Cosmopolitan phyla were more abundant than endemic ones, with the exceptions for GG01, SYNH02, and SH01. Proteobacteria appears to be the only phylum present in all 136 samples (and all MVs) and the most abundant phylum in nearly all MVs (except for GG01 and SI02). Whereas the remaining eight phyla were present in all MVs, they were absent in few samples and occurred in 124 to 345 135 samples. The proportions of cosmopolitan taxonomic units decreased from the level of phylum to ASV (Fig. 3b – 3e). Among the detected 1,214 genera, the genus *Desulfurivibrio* was the most abundant one and present in 98 of the 136 samples. Two other prevalent genera were detected in 126 samples and taxonomically assigned to the unclassified genera related to Anaerolineae within Chloroflexi and to Gammaproteobacteria, respectively.

350 At the ASV level, no truly cosmopolitan ASVs were identified (Fig. 3f). Pairwise comparisons yielded a shared 0–15.4% and 0–51.3% of the ASVs between MVs and between samples, respectively. In particular, the communities at SI02 completely differed from AK03, SM22, and LGH03. The most widely distributed ASVs were present in 9 MVs (Fig. 3f & Table S2) and constituted only 0.4% of the total sequences. Their sequences were affiliated with either the unclassified genus of Desulfuromonadaceae or *Desulfotignum*. Compared with the pattern based on higher taxonomic units (between genus and class), the ASVs confined at one MV and less than/equal to three MVs constituted 85% and 99% of the total ASVs, respectively, and were taxonomically diverse and unevenly abundant. Detailed information for the 10 most abundant ASVs is given in Table S2.

Deleted: number of

Deleted: demonstrated

Deleted: patterns

Deleted: fully

Deleted: .

Deleted: % (Fig. 2b).

Deleted: constitute

Deleted: Most

Deleted: %). The

Formatted: Tab stops: 4.25 cm, Left

Deleted: .

Deleted: In most MVs, the abundances of cosmopolitan

Deleted: higher

Deleted: The

Deleted: 1214

Deleted: out of the 136

Deleted: ). Although these ASVs

Deleted: , their

Deleted: In contrast to

Deleted: of phyla or genera.

Deleted: 30

Deleted: were restricted to one to three cores



Within individual cores, the number of phyla ranged from 12 (SI02) to 62 (PA01). Although 16.1% (PA01)–58.5% (AR01) of detected phyla were shared between samples within individual cores, 6.3–40% of phyla were restricted to single samples. Similar to the pattern for phyla, the lowest number of genera occurred at SI02 (52), whereas the highest number was present at PA01 (550). In addition, 3.4% (GG01) to 26.5% (AR01) of genera, and up to 13.2% (SI02) of ASVs were shared within individual cores. In contrast, up to 49.9% (PA02) of genera and 83.9% (GG01) of ASVs were restricted to a single sample. Overall, community dissimilarities appear to be more pronounced between samples from distinct MVs than from within the individual MVs, indicating a high degree of endemism (Fig. 4a).

**Deleted:** between  
**Deleted:** of  
**Deleted:** %–  
**Deleted:** of  
**Deleted:** depth  
**Deleted:** dissimilarity appears

385

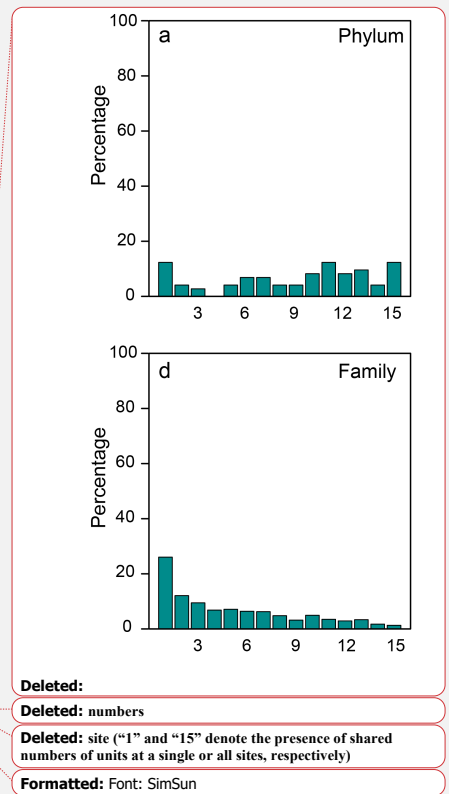
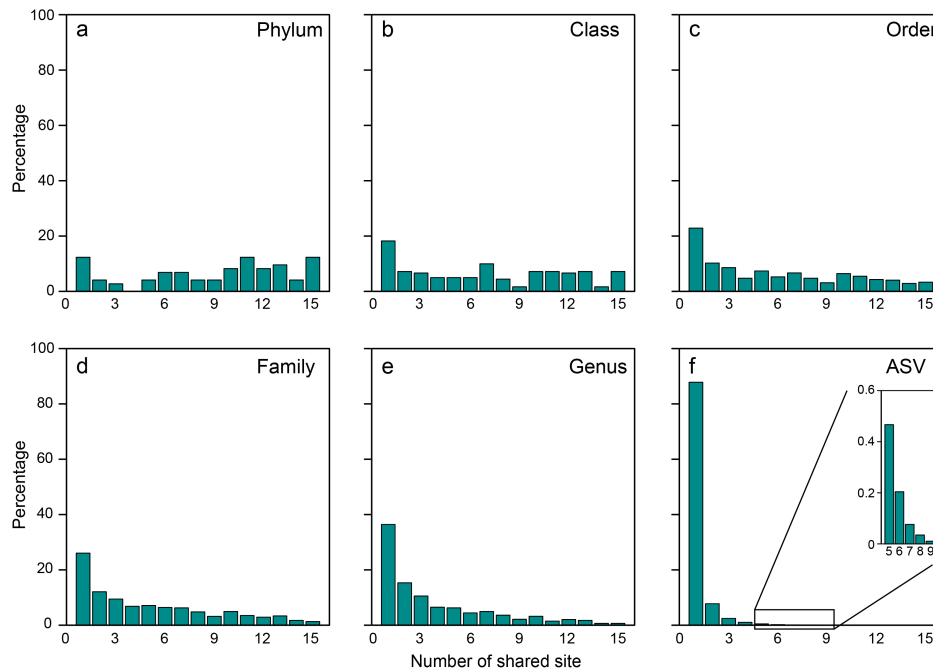
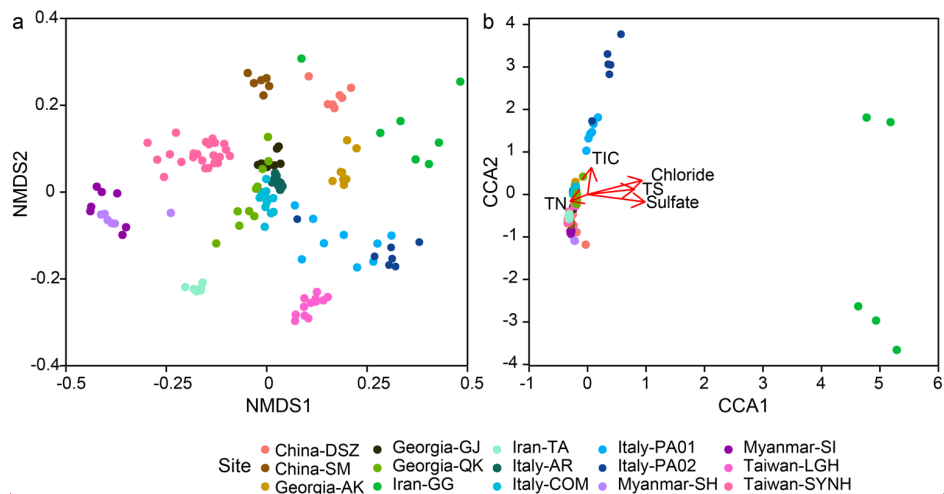


Figure 3: Proportions of specific taxonomical units shared between the number of MVs. (a) phylum, (b) class, (c) order, (d) family, (e) genus, and (f) ASV.



400 **Figure 4: Variance of 16S rRNA community compositions deduced from (a) the NMDS analysis based on the Bray-Curtis distance and (b) the CCA analysis based on the Chi-square distance. Ordination of significant geochemical parameters was overlaid for comparison in (b).**

### 3.3 Environmental effects

405 Multiple regression analysis yielded that methane, TN, and TIC concentrations had meaningful contributions (summed to be 18.8%) to the Shannon index (Table S3), with TIC being the most influential one (13.4% linear regression,  $P < 0.001$ ; Table S4). Similarly, the TIC concentration was also significantly correlated with the Shannon index (Pearson's coefficient:  $|r| = 0.38$ ,  $P < 0.001$ ; Figure S6).

410 Community dissimilarities were correlated more strongly with chloride (Mantel:  $\rho = 0.45$ ,  $P < 0.001$ ) than with sulfate (Mantel:  $\rho = 0.26$ ,  $P < 0.001$ ) concentrations and other geochemical parameters (Table S5). Permutational multivariate analysis of variance in community assemblage showed that TIC (3.6%) and TN (3.1%) concentrations had the highest contribution to the beta diversity, followed by sulfate (2.9%) and chloride (2.6%), TOC (2.4%), TS (2.0%), and methane concentrations (0.9%) ( $P < 0.001$ ; Table S6).

415 The CCA yielded that the eight environmental parameters combined (sample depth, and concentrations of chloride, sulfate, and methane, TIC, TOC, TN, and TS) explained 12% of community dissimilarity (Fig. 4b). Of these factors, chloride, sulfate, TIC, TS, and TN significantly contributed to the overall differences in community composition. For communities within individual cores, a combination of various factors described above was significantly correlated with community dissimilarities

Formatted: English (US)

Formatted: English (US)

Deleted: Community dissimilarity revealed by (a) non-metric multidimensional scaling and (b) constrained correspondence analyses on ...

Deleted: gene amplicons. Community relatedness was quantified by ...

Deleted: .

Deleted: plotted

Deleted:

Deleted: showed

Deleted: concentrations of

Deleted: S2

Deleted: S3

Deleted: dissimilarity was

Deleted: S4

Deleted: towards

Deleted: S5

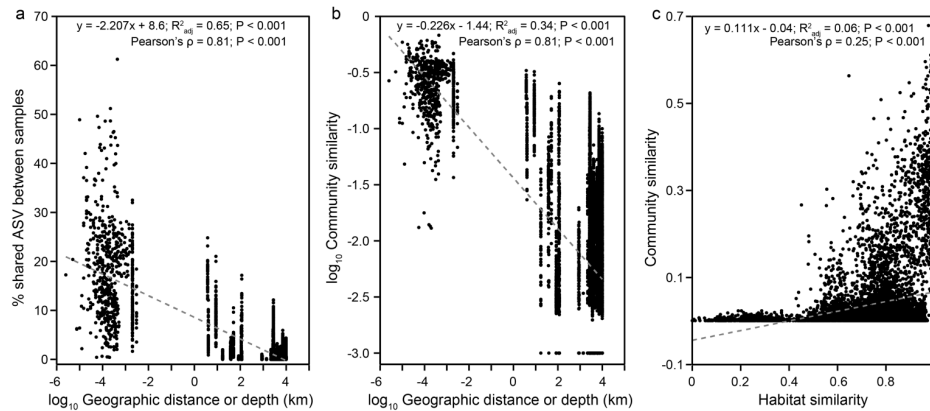
Deleted: sampling

Deleted: dissimilarity

435 (Figure S7). For example, the depth factor was significant for the community dissimilarities within 11 out of 16 individual  
 440 cores. In contrast, the chloride factor was only significant for the community dissimilarities within two individual cores (QK01  
 and SYNH02C4). Finally, none of the selected factors were significantly correlated with the community dissimilarities within  
 445 TA01, SH01, SI01, SM22, and LGH03.

### 3.4 DDR and NST patterns

440 Community structure varied widely across a scale of 9,924 km (Bray-Curtis  $R_{ANOSIM} = 0.967$ ,  $P < 0.001$ ; Figure S8). Both the  
 proportions of shared ASVs and community similarities significantly decreased with increasing geographical distance (Mantel:  
 $\rho = -0.80$ ,  $P < 0.001$ ), indicating a significant DDR with a slope coefficient,  $|\beta_1|$ , of 0.226 ( $P < 0.001$ ) (Figs. 5a & b). If only  
 communities from individual cores were considered, a DDR (Mantel:  $\rho = 0.65$ ,  $P < 0.001$ ) with an even higher  $|\beta_1|$  value of  
 0.241 was obtained (Figures S9b). Close examinations revealed that similarities of communities distributed within individual  
 445 cores were not significantly correlated with distance (or depth; Figures S9d & e). Such variations in DDR reveal that  
 community compositions were controlled by different mechanisms at vertical versus horizontal scales. Furthermore, the  
 NST<sub>bray</sub> values varied from 100% for “bubbling fluid”, 100% for “surface sediment”, to between 0.89% and 62.54% for “within  
 MV sediment” (Table S1). For “within MV sediment” category, the NST<sub>bray</sub> values for 12 out of 15 MVs were less than 50%  
 (Table S1). For comparison, the same NST<sub>Jaccard</sub> values for “bubbling fluid” and “surface sediment”, and a similar NST<sub>Jaccard</sub>  
 450 range for “within MV sediment” (1.01% – 60.90%) were obtained (Table S1). The pattern for pNST values resembled those  
 for NST<sub>bray</sub> and NST<sub>Jaccard</sub> values (Supplementary information: Table S1).



Deleted: dissimilarity

Deleted: dissimilarity

Deleted: dissimilarity

Deleted: Distance decay relationship

Deleted: -

Deleted: proportion

Deleted: ASV

Deleted: similarity

Commented [Office4]: Check the value >

Deleted: (Figs.

Moved down [1]: 5a & b).

Deleted: The

Deleted: for the distance decay relationship

Deleted: was

Deleted: 210

Moved (insertion) [1]

Deleted: ).

Deleted: separate

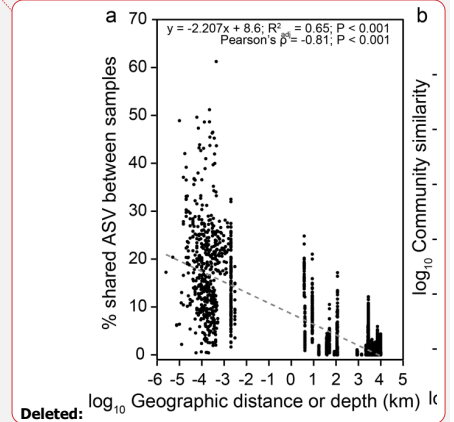
Deleted: !

Formatted: Not Highlight

Commented [Office5]: 0.24

Deleted: 225

Formatted: Not Highlight



Deleted: log<sub>10</sub> Geographic distance or depth (km)

475 **Figure 5: Biogeographic patterns for microbial communities. Plots of (a) proportion of shared ASV and (b) community similarity versus geographic distance or depth, and (c) community similarity versus habitat similarity, based on pairwise comparison for a total of 126 samples.**

## 4 Discussion

### 4.1 Environmental selection in terrestrial mud volcanoes

480 This study recovered diverse and complexly structured microbial communities in terrestrial MVs distributed across the Eurasian continent. Further linear regression analyses yielded that the Shannon index was mostly controlled by TIC (Figure S6 and Tables S3–S4). Both the Mantel test and CCA revealed that community similarities were strongly influenced by chloride, sulfate, TIC, and TS concentrations (Fig. 4b and Table S5) and correlated with habitat similarities (Fig. 5c and Figure S10). To explore the controlling factors for community variance further, the individual factors stated above were addressed at the community level first, followed by at the level of specific, abundant lineage.

485 Salinity has been identified as the primary factor shaping the distribution of microorganisms (Or et al., 2007). Because chloride is inert to most catabolic and abiotic reactions, any correlation between community (Or et al., 2007) index and chloride concentration could have reflected the physiological response or tolerance to salinity variation (Or et al., 2007) related to evaporation and evaporite dissolution/precipitation. Chloride concentrations measured in this study spanned over a broad range between 82 and 4890 mM. Whereas the community similarity was shaped by chloride (Fig. 4b and Supplementary Table S5), the abundances of specific lineages, including Haloferacaceae and Halobacteriaceae within Halobacteria, were also significantly correlated with the chloride concentrations (Figure S10). In particular, the order Halobacteria detected in 11 out of the 15 investigated MVs was highly enriched in hypersaline MVs (GG01, PA01, and PA02) where the chloride concentrations reached up to 4890 mM. Previous culture tests have shown that strains affiliated with this lineage can cope with the stress imposed by high osmotic pressures and low water activities (Grant, 2004). All members of the family Halobacteriaceae grow optimally at chloride concentrations of above 2500 mM (Oren, 2014) and up to 5000 mM (Halobacterium sp. NRC-1) (DasSarma and DasSarma, 2001). In contrast, the abundances of JS1 within Atribacteria and Hydrogenophilaceae within Proteobacteria were negatively correlated with the chloride concentrations ( $\rho < -0.5$ ; Figure S10). Although these two families were prevalently distributed in all MVs, the correlation pattern suggests their sensitive response to the salinity stress and preference for low salt conditions.

495 TIC in sedimentary systems represents a pool of biological carbonate remains and authigenic carbonate formed or induced by microbial processes (Zheng et al., 2011). Considering that carbonate fossils are exempted from the preservation of genetic materials during burial diagenesis (Allison and Pye, 1994), the correlation between TIC and community similarity could have been controlled by the composition of heterotrophs and methanotrophs capable of converting organic carbon and methane into dissolved carbonate and eventually to the precipitation of carbonate minerals. Therefore, the presence and concentration of TIC might reflect microbial capability for the utilization of organic carbon or methane to some degrees. In addition to the

**Deleted:** Geographic

**Formatted:** English (US)

**Deleted:** Proportion

**Formatted:**

[... [8]

**Formatted:** English (US)

**Deleted:** .

**Deleted:** Plot of

**Formatted:** English (US)

**Deleted:** . Each dot represents the difference

**Formatted:** English (US)

**Formatted:** English (US)

**Deleted:** paired samples (with

**Formatted:** English (US)

**Deleted:** ).

**Formatted:** English (US)

**Deleted:** The diversity...his study recovered diverse and composition of...

[... [9]

**Formatted:** Font: PMingLiU

**Deleted:** from geographically separated

**Formatted:** Font: +Body (Times New Roman)

**Deleted:** environments...istributed across the Eurasian Continent were characterized. Linear...ontinent. Further linear regression analyses yielded that the Shannon index was mostly controlled by TIC (Figure S6 and Tables S2...3–S4). Both the Mantel test and CCA revealed that community similarity was...imilarities were strongly influenced by chloride, sulfate, TIC, and TS concentrations (Fig. 4b and Table S4)...5) and correlated with habitat similarity...imilarities (Fig. 5c and Figure S10). To explore more about ...

[... [10]

**Deleted:** S4...5), the abundances of specific lineages, including Haloferacaceae and Halobacteriaceae within Halobacteria, were also significantly correlated with the chloride concentrations (Figure S10). In particular, the order Halobacteria detected in 11 out of the 15 sampled terrestrial...investigated MVs was highly enriched in hypersaline MVs, including ... (GG01, PA01, and PA02, ...

[... [11]

**Formatted:** Font color: Black, English (UK)

**Deleted:** from...r induced by microbial degradation of organic matter and methane oxidation

[... [12]

**Formatted:** Font color: Black, English (UK)

**Deleted:** ).

**Formatted:** Font color: Black, English (UK)

**Deleted:** or...r and methane into dissolved carbonate and eventually to the precipitation of carbonate minerals. Therefore, the presence and the ...oncentration of TIC might reflect the ...icrobial capability for the utilization of organic carbon or methane at...o some degrees. The ability to respire organic carbon or methane is widely embedded among diverse microorganisms (Cherrier et al., 1996).

[... [13]

community variance, the abundances of a variety of families, such as Woesearchaeia, Thiohalorhabdaceae, Marinilabiliaceae, 570 Lentimicrobiaceae, Haloferaceae, Halobacteriaceae, Ectothiorhodospiraceae, Desulfarcularaceae, Balneolaceae, and Anaerolineaceae were found to be significantly correlated with the TIC concentrations (Figure S10). Whereas none of the methanotrophs are related to the lineages described above, previous studies have demonstrated that a large number of strains affiliated with Halobacteriales, Marinilabiliaceae, Lentimicrobiaceae, Desulfarcularales, and Anaerolineaceae are capable of metabolizing various forms of organic carbon (e.g., fatty acids, sugars, amino acids, hydrocarbons, and even short-chain alkanes) (Yamada and Sekiguchi, 2009; McGenity, 2010; Kuever, 2014; McIlroy and Nielsen, 2014; Borrel et al., 2019; Mori et al., 2019). Moreover, metagenomes with 16S rRNA gene sequences affiliated with Woesearchaeota contain genes for starch/sugar utilization, glycolysis, folate C1 metabolism, and fermentation (Liu et al., 2018). The gene pattern further suggests the heterotrophic nature of Woesearchaeota and its potential requirement of metabolic complement from other microorganisms (e.g., acetate-utilizing methanogens). Overall, the physiological characteristics derived from previous cultivation experiments, 580 along with metagenomic data, all demonstrate the prevalence of heterotrophy among these phyla/orders. The positive correlation between their abundances and TIC concentration suggests a connection between carbon utilization and carbonate precipitation. We noted that a similar pattern was not observed for TOC and TN (Table S5). It is likely that the pools of bioavailable and biodegradable TOC and TN only constitute a small fraction of the pool size, thereby rendering TOC and TN less sensitive to the community variance.

585 Compared with chloride, sulfate concentrations varied at a higher magnitude (the CV of 13–186%; Table S7). With the exception of SH01 and SYNH02, the sulfate concentrations were not significantly correlated with the chloride concentrations (Table S7). The decoupling of sulfate from chloride suggests that in addition to the evaporation or dissolution/precipitation of evaporite minerals, microbially mediated sulfate reduction or oxidation of reduced sulfur plays a role in controlling sulfate abundance. Whereas the sulfate concentrations were significantly correlated with the community similarities (Table S5), 590 abundant sulfur oxidizers and sulfate reducers (such as Hydrogenophilaceae, Desulfobulbaceae, and Desulfuromonadaceae related members; Or et al., 2007) were detected at SI02, SH01, and AR01. In addition, the abundances of sulfur-metabolizing lineages, such as sulfur-oxidizing *Thiobacillus* members within Hydrogenophilaceae ( $\rho = 0.38, P < 0.001$ ) and sulfate-reducing members related to Desulfobulbaceae and Desulfarcularaceae ( $\rho = -0.40, P < 0.001$ ; Figure S10), were found to be significantly correlated with the sulfate concentrations.

595 Similar to TIC, TS represents an aggregation of various sulfur-bearing minerals formed through different processes at varying time scales. These pools of minerals include pyrite (or other sulfide minerals) and gypsum precipitated over geological time, and sulfide minerals (e.g., iron monosulfide and pyrite) produced from microbial sulfate reduction at a contemporary time scale (Halevy et al., 2012). In contrast to marine environments where the sulfate pool is enormous, terrestrial MVs are often devoid of sulfate, unless evaporite is ubiquitous. Therefore, in situ sulfate reduction proceeds with sulfate produced from microbial sulfur oxidation or gypsum dissolution (Canfield, 1989; Yao and Millero, 1996; Weber et al., 2017). In this regard, 600 the correlation between TS and community similarity observed in this study demonstrated that in situ microbial processes played a role in shaping community compositions. Detailed analyses further revealed that the abundances of a variety of

**Deleted:** concentration

**Deleted:** While

**Deleted:** heterotrophs,

**Formatted:** Font color: Black, English (UK)

**Deleted:** In addition, molecular analyses reveal that

**Formatted:** Font color: Black, English (UK)

**Deleted:**

**Deleted:** abundance

**Deleted:** S4

**Deleted:** total

**Deleted:** S6

**Deleted:** for most sites

**Deleted:** S6

**Deleted:** play

**Deleted:** abundances

**Deleted:** concentration was

**Deleted:** similarity

**Deleted:** S4

**Deleted:** ,

**Deleted:** ,

**Deleted:** ) (

**Deleted:** from various samples

**Deleted:** significant correlations between the abundance

**Deleted:** (e.g.,

**Deleted:** ) and sulfate concentration were observed. Whereas ANME-2a could not directly reduce sulfate, their syntrophic partners (e.g., sulfate-reducing bacteria affiliated with Deltaproteobacteria) reduce sulfate by the electrons derived from methane oxidation (McGlynn et al., 2015); the relative abundance of ANME-2a represented a negative correlation with sulfate concentration ( $\rho = -0.54, P < 0.001$ ; Figure S10).

**Deleted:** ,

**Formatted:** Font color: Black, English (UK)

**Formatted:** Font color: Black, English (UK)

**Formatted:** Font: Not Italic, Font color: Black, English (UK)

**Formatted:** Font color: Black, English (UK)

families, such as Thiohalorhabdaceae, Balneolaceae, and Haloferaceae, were positively correlated with the TS concentrations (Supplementary Figure S10). Among these families, most strains affiliated with Thiohalorhabdaceae can directly metabolize sulfur (Sorokin et al., 2020). In contrast, the abundances of lineages, such as Methanosaetaceae, Marinobacteraceae, Methylomonaceae, and JS1, were negatively correlated with the TS concentrations. Although these lineages have been commonly observed at the sulfate-to-methane transition in marine sediments (Orphan et al., 2001; Inagaki et al., 2006), the correlation pattern suggests their proliferation in sulfur-depleted environments.

Methane has been found to be abundant in most MVs (Etiope et al., 2019), providing an energetic substrate and carbon source for various metabolisms. Its abundances varied substantially (CV of 277%) and were neither correlated with the chloride concentrations nor community similarities. Previous studies have demonstrated that carbon isotopic compositions and C1 / (C2 + C3) abundance ratios could be used to distinguish methane produced from methanogenesis from thermal maturation (Whiticar, 1999). Thermogenic hydrocarbon gases generally possess C1 / (C2 + C3) abundance ratios ranging from 0 to 50 and carbon isotopic compositions of methane greater than -50‰ (Claypool and Kvenvolden, 1983), whereas microbial sources generate hydrocarbons with C1 / (C2 + C3) abundance ratios generally greater than 1000 and carbon isotopic compositions of methane smaller than -60‰ (Claypool and Kvenvolden, 1983). Regardless of the production source, microbial methane consumption would impart carbon isotopes of methane, preferentially producing <sup>13</sup>C-enriched CO<sub>2</sub> or leaving residue methane enriched with <sup>13</sup>C.

In this study, rather than community dissimilarity, the abundances of methanogens (members of Methanosaetaceae) were significantly correlated with the methane concentrations ( $\rho = 0.23$ ,  $P < 0.001$ ; Figure S10). Although both C1 / (C2 + C3) abundance ratios and carbon isotopic compositions of methane revealed a mixed origin of methane (Supplementary Figures S2 & S3), the correlation pattern supports a quantitative role of microbial over thermogenic methane production in terrestrial MVs. Furthermore, both aerobic and anaerobic methanotrophs were detected in 11 of the 15 investigated MVs. Whereas these two types of methanotrophs possess contrasting oxygen affinities, they were all distributed from the surface to the bottom of investigated cores. Resembling the findings in the marine setting (Ruff et al., 2015), neither the abundances of the entire ANME (Figures S10) nor the community dissimilarities were significantly correlated with the methane concentrations. The abundances of the whole ANME and ANME-2a/b were inversely correlated with the carbon isotopic compositions of methane and sulfate concentrations ( $\rho = -0.37$  and  $-0.32$  for whole ANME,  $P < 0.001$ ;  $\rho = -0.42$  and  $-0.45$  for ANME-2a/b,  $P < 0.001$ ), respectively, a pattern consistent with the coupling of methane oxidation with sulfate reduction mediated by ANME-2a/b and Delta-Proteobacteria (Knittel and Boetius, 2009). In addition, ANME-2d related sequences were mostly distributed at LGH03. Previous culture and field studies have shown that ANME-2d related members can oxidize methane with the reduction of nitrate, iron, and manganese (Beal et al., 2009; Haroon et al., 2013; Ettwig et al., 2016; Scheller et al., 2016). Our findings suggest that anaerobic methanotrophy driven by electron acceptors other than sulfate is not prevalent in terrestrial MVs.

Finally, the factor of depth represents an integration of geochemical variations (e.g., sulfate, methane, and chloride). The counteraction between the downward penetration of atmospheric oxygen and upward migration of reducing methane would presumably result in a steep redox gradient along the depth (Lin et al., 2018), leading to a segregation of distinct niches with

- Deleted:** significantly
- Deleted:** concentration
- Deleted:** Most
- Formatted:** Font color: Black, English (UK)
- Formatted:** Font color: Black, English (UK)
- Deleted:** ). Their negative correlations with TS suggest
- Deleted:**
- Deleted:** Furthermore, methane was
- Deleted:** the studied
- Deleted:** ,
- Deleted:** dissimilarity
- Formatted:** Font color: Black, English (UK)
- Deleted:** In this regard, thermogenic
- Deleted:** C1
- Formatted:** Font color: Black, English (UK)
- Deleted:** C1
- Deleted:**
- Deleted:** abundance
- Deleted:** was
- Deleted:** concentration
- Formatted:** Font color: Black, English (UK)
- Deleted:** abundance
- Deleted:** dissimilarity
- Deleted:** concentration.
- Deleted:** overall
- Deleted:** overall
- Formatted:** Font color: Black, English (UK)
- Deleted:** -
- Formatted:** Font color: Black, English (UK)
- Deleted:** methanotrophy

690 community compositions adapted to various redox and geochemical affinities. Indeed, the within-core community similarity was significantly correlated with depth for 11 cores (Figure S7) and with habitat similarity for all cores (Figure S9), a pattern consistent with what has been reported for marine sediments (Jorgensen et al., 2012; Ruff et al., 2015; Petro et al., 2017).

#### 4.2 Microbial dispersal patterns

695 A distance–decay trend was identified for geographic distances up to ~10,000 km (Figs. 1, 2, and 5). The deduced  $\beta_1$  value (0.226) was smaller than that for macro-organisms ( $\beta_1 = 0.2–0.7$ ) (Nekola and White, 1999), pointing to a higher dispersal rate of microorganisms (Astorga et al., 2012; Zinger et al., 2014). Furthermore, the  $\beta_1$  value resembled those for microbial communities in coastal sediments (Zinger et al., 2014) and was larger than those ( $\beta_1 = 0–0.15$ ) for microbial communities in marine seeps and MVs (Ruff et al., 2015), and seawater columns (Zinger et al., 2014), suggesting a higher degree of dispersal limitation in terrestrial and transition zone sediments than in marine environments. Our results are in contrast to the biogeographic pattern derived from ammonia-oxidizing bacteria in salt marsh sediments where dispersal limitation at the local scale contributes to the beta diversity, and no evidence of evolutionary diversification is observed at the continental scale (Martiny et al., 2011). Furthermore, the mean NST values for both “bubbling fluid” and “surface sediment” categories were high (100%) (Table S1). These sample categories represent either deeply sourced communities (for “bubbling fluid”) or source communities susceptible to the alteration of surface processes (for “surface sediment”). Considering that most of these MVs are distant from each other (except for SI01 and SH01), fluid exchange and subsequently microbial dispersal or exchange between MVs could be exempted. Therefore, the high NST values associated with these two categories suggest that highly stochastic control on community variance is likely linked to the limitation imposed by distance separation. In contrast, the mean NST value for “within MV sediment” category was 32%. The NST values were < 50% for 12 out of 15 MVs and between 59% and 63% for the remaining three MVs. This sample category represents a suite of sediments successively buried with depth by the mud emanating from bubbling pools or cones. With the counteraction of atmospheric oxidation and reducing power derived from methane, sulfur, and organic matter, a strong redox and geochemical gradient develops as a result of the transient interaction between biogeochemical cycling and abiotic processes (Chang et al., 2012; Cheng et al., 2012; Wang et al., 2014; Tu et al., 2017; Lin et al., 2018). Therefore, the relatively low NST values suggest that the deterministic control on within-MV-community variance is predominantly impacted by the localized redox and geochemical context that is tightly linked to the channeling of mud and fluid sourced to the deep reservoirs.

715 Of diverse community members possessing key methane and sulfur metabolisms, ANME, Desulfobacterales, Methylococcales, and *Thiobacillus* were identified as the cosmopolitans, being present in 9–13 of the investigated MVs. The most abundant ANME ASV (accounting for 7.9% of all ANME sequences) appeared to be the most dominant one at LGH03 (2.2% of the total reads) but was present only as a few sequences at TA and PA01 (less than 0.1% at each MV). The most widespread ANME ASV was observed at 5 MVs in Italy and Georgia (Figure S11), although it only represented 0.8% of all ANME sequences. A similar pattern was observed for the most abundant ASVs of the Desulfobacterales and *Thiobacillus* that

Deleted: ),

Formatted: Font color: Black, English (UK)

Deleted: Starnawski

Formatted: Font color: Black, English (UK)

Formatted: English (US)

Deleted: distance across the Eurasian continent

Formatted: Font color: Text 1

Formatted: Font color: Text 1

Deleted: 210) deduced

Deleted: ). Such a feature could be attributed

Formatted: Font color: Black, English (UK)

Deleted: ,

Formatted: English (US)

Formatted: Font color: Black, English (UK)

Deleted: ).

Deleted: at

Deleted: sampled

Deleted: at LGH03

Deleted: were

Deleted: site

Deleted: ASV

735 represented 2% and 11% of individual lineages but ~~were~~ only present at 2 and 4 MVs, respectively. The most widespread  
 740 ~~ASVs~~ of these lineages (Figure S11) ~~were~~ observed at 9 MVs and only accounted for 0.3% of individual lineages. Comparisons  
 with marine counterparts further revealed a higher degree of endemism for terrestrial MVs (Fig. 3; ~~88%~~ and 70% of ASVs  
 unique to one terrestrial and marine MV, respectively) (Kahle and Wickham, 2013) and drastically different community  
 compositions mediating some of these key metabolisms. For example, sulfide-oxidizing Thiotrichales and methanotrophic  
 ANME-1 and ANME-3 ~~are~~ prevalent in marine settings (Ruff et al., 2015). This finding is in contrast to the terrestrial  
 cosmopolitan sulfur-oxidizing *Thiobacillus* and methanotrophic ANME-2a reported in this study.

Overall, the high  $|\beta|$  ~~and NTS values~~ (Fig. 5), together with the high level of endemism in terrestrial MVs, ~~reflect~~ a strong  
 pressure for local diversification. In terrestrial MVs, reduced materials are expelled to and distributed in a limited extent of the  
 surface environment. A strong redox gradient is generated across a transect from the center of MVs to the surrounding region,  
 745 (~~Chang et al., 2012; Cheng et al., 2012; Wang et al., 2014; Tu et al., 2017; Lin et al., 2018~~). This phenomenon, combined with  
 the lack of subsurface fluid exchange between terrestrial MVs, suggests that microbial dispersal is only facilitated through air  
 circulation. Such a route imposed by strong oxidative power would be, however, particularly detrimental to further colonization  
 of anaerobes ~~in~~ destination MVs. Exceptions analogous to the dispersal of thermophilic anaerobes from marine hydrothermal  
 vents might occur if a protective agent, such as germination or sporulation, could be developed to cope with the stress  
 750 associated with ~~the~~ exposure to the air (Bray and Curtis, 1957; Müller et al., 2014). The limitation in dispersal also renders  
 terrestrial MVs a habitat patchily distributed and bears limited genetic exchange with the surrounding habitats.

**Deleted:** was

**Deleted:** ASV

**Deleted:** was

**Deleted:** 80

**Formatted:** Font color: Black, English (UK)

**Deleted:** were

**Deleted:** value

**Deleted:** )

**Deleted:** reflects

**Deleted:** .

**Deleted:** at

**Formatted:** Font color: Black, English (UK)

**Formatted:** Font color: Black, English (UK)

**Formatted:** English (US)

**Deleted:** , including

**Deleted:** from

**Deleted:** sites

**Deleted:** similarity

**Deleted:** distance

**Deleted:** similarity

**Deleted:** greater

**Deleted:** is

**Deleted:** some

**Deleted:** value

**Deleted:** 80

**Deleted:** environmental

## 5 Conclusions

We reported microbial community diversities and compositions associated with terrestrial MVs across the Eurasian continent.  
 At a higher taxonomic level (phylum to order), a rather uniform composition of microbiomes was recovered from most MVs.  
 755 ~~The major phyla recovered included~~ Proteobacteria, Chloroflexi, Euryarchaeota, Cyanobacteria, Firmicutes, Atribacteria,  
 Bacteroidetes, and Actinobacteria. In contrast, abundant ASVs (a total of 28,928) were unevenly detected ~~in~~ various MVs,  
 among which no true cosmopolitan ASV was found. Community ~~similarities~~ decreased and increased with geographic  
~~distances~~ and habitat ~~similarities~~, respectively. ~~Although high NST values (100%) were observed for “bubbling fluid” and~~  
 760 ~~“surface sediment” communities, low NST values (< 50%) were derived for “within MV sediment” in 12 out of 15 MVs.~~ The  
 slope of the DDR was ~~steeper~~ than those for marine MVs, seeps, and water columns. Such community relatedness ~~was~~  
 significantly correlated with ~~various~~ physiochemical parameters, such as chloride, TIC, methane, and sulfate. Within individual  
 cores, the significant correlation between community and habitat similarities highlights the importance of environmental  
 filtering at a localized, vertical scale. In summary, the high  $|\beta|$  ~~and NST values~~ combined with ~~85%~~ of ASVs confined to  
 individual MVs suggest the limit in microbial dispersal capability and a high degree of endemism. Such stochastic processes  
 765 operating at continental scales in addition to ~~deterministic~~ filtering at local scales drive the formation of patchy habitats and  
 the pattern of diversification in terrestrial MVs.



790 **Acknowledgments**

We are grateful to the anonymous reviewers for their constructive and critical comments, and a number of scientists for their assistance in the field sampling. We want to offer special thanks to Prof. Sun-Lin Chung at Academia Sinica, Taiwan for his initiation and coordination of logistic arrangement for field works in Central Asia. This work was supported by the Ministry of Science and Technology (NSC 100-2627-M-002-003; MOST 109-2116-M-002-015; MOST 109-2116-M-110 -001 -MY3) and the Ministry of Education, Taiwan.

**Author contributions**

LHL and PLW initiated and designed the study. YPC, LHL, LWW, FI, JBHS, and SNR performed field works. THT, LLC, YPC, LHL, LWW, and PLW performed laboratory and statistical analyses. All participated the discussion and paper writing.

800 **References**

Allison, P. A. and Pye, K.: Early diagenetic mineralization and fossil preservation in modern carbonate concretions, *Palaios*, 9, 561–575, <https://doi.org/10.2307/3515128>, 1994.

805 Astorga, A., Oksanen, J., Luoto, M., Soininen, J., Virtanen, R., and Muotka, T.: Distance decay of similarity in freshwater communities: Do macro- and microorganisms follow the same rules?, *Glob. Ecol. Biogeogr.*, 21, 365–375, <https://doi.org/10.1111/j.1466-8238.2011.00681.x>, 2012.

Beal, E. J., House, C. H., and Orphan, V. J.: Manganese- and iron-dependent marine methane oxidation, *Science*, 325, 184–187, <https://doi.org/10.1126/science.1169984>, 2009.

810 Bolyen, E., Rideout, J., Dillon, M., Bokulich, N., Abnet, C., Al-Ghalith, G., Alexander, H., Alm, E., Arumugam, M., Asnicar, F., Bai, Y., Bisanz, J., Bittinger, K., Brejnrod, A., Brislawn, C., Brown, C., Callahan, B., Caraballo-Rodriguez, A., Chase, J., Cope, E., Silva, R., Dorrestein, P., Douglas, G., Durall, D., Duvallet, C., Edwardson, C., Ernst, M., Estaki, M., Fouquier, J., Gauglitz, J., Gibson, D., Gonzalez, A., Gorlick, K., Guo, J., Hillmann, B., Holmes, S., Holste, H., Huttenhower, C., Huttley, G., Janssen, S., Jarmusch, A., Jiang, L., Kaehler, B., Kang, K., Keefe, C., Keim, P., Kelley, S., Knights, D., Koester, I., Kosciolk, T., Kreps, J., Langille, M., Lee, J., Ley, R., Liu, Y., Loftfield, E., Lozupone, C., Maher, M., Marotz, C., Martin, B., McDonald, D., McIver, L., Melnik, A., Metcalf, J., Morgan, S., Morton, J., Naimey, A., Navas-Molina, J., Nothias, L., Orchanian, S., Pearson, T., Peoples, S., Petras, D., Preuss, M., Pruesse, E., Rasmussen, L., Rivers, A., II, M., Rosenthal, P., Segata, N., Shaffer, M., Shiffer, A., Sinha, R., Song, S., Spear, J., Swafford, A., Thompson, L., Torres, P., Trinh, P., Tripathi, A., Turbaugh, P., Ul-Hasan, S., Hoof, J., Vargas, F., Vázquez-Baeza, Y., Vogtmann, E., Hoppel, M., Walters, W., Wan, Y., et al.: QIIME 2: Reproducible, interactive, scalable, and extensible microbiome data science. *PeerJ Prepr.*, 6, e27295v2, <https://doi.org/10.7287/peerj.preprints.27295v2>, 2018.

820 Borrel, G., Adam, P. S., McKay, L. J., Chen, L.-X., Sierra-García, I. N., Sieber, C. M. K., Letourneur, Q., Ghazlane, A., Andersen, G. L., Li, W.-J., Hallam, S. J., Muyzer, G., Oliveira, V. M. de, Inskeep, W. P., Banfield, J. F., and Gribaldo, S.: Wide diversity of methane and short-chain alkane metabolisms in uncultured archaea, *Nat. Microbiol.*, 4, 603–613, <https://doi.org/10.1038/s41564-019-0363-3>, 2019.

Formatted: English (US)  
Formatted: Font: 10 pt, Font color: Black, English (UK)  
Formatted: [14]  
Deleted: preservation  
Formatted: [15]  
Formatted: csl-entry  
Deleted: (6),  
Formatted: [16]  
Deleted: :  
Formatted: Font: 10 pt, Font color: Black, English (UK)  
Deleted: do  
Formatted: [17]  
Deleted: :  
Formatted: Font: 10 pt, Font color: Black, English (UK)  
Deleted: Science,  
Formatted: Font: 10 pt, Font color: Black, English (UK)  
Deleted: (5937),  
Formatted: [18]  
Formatted: [19]  
Deleted: :  
Formatted: Font: 10 pt, Font color: Black, English (UK)  
Deleted: Bolyen, E., Rideout, J.R., Dillon, M.R. et al.: Reproducible, interactive, scalable and extensible microbiome data science using QIIME 2, *Nat. Biotechnol.*, 37, 852–857, doi: 10.1038/s41587-019-0209-9, 2019.  
Formatted: Font: 10 pt, Font color: Black, English (UK)  
Formatted: csl-entry  
Formatted: [20]  
Moved (insertion) [2]  
Formatted: Font: 10 pt, Font color: Black, English (UK)  
Deleted: M.K., et al  
Formatted: Font: 10 pt, Font color: Black, English (UK)  
Deleted: :  
Formatted: [21]  
Deleted: :  
Formatted: Font: 10 pt, Font color: Black, English (UK)

855	Bray, J.R. and Curtis, J.T.: An ordination of the upland forest communities of southern Wisconsin, <i>Ecol. Monogr.</i> , 27, 325–349, 1957.	Formatted ... [22] Deleted: doi: 10.2307/1942268,
	Canfield, D.E.: Reactive iron in marine sediments, <i>Geochim. Cosmochim. Acta</i> , 53, 619–632, <a href="https://doi.org/10.1016/0016-7037(89)90005-7">https://doi.org/10.1016/0016-7037(89)90005-7</a> , 1989.	Formatted ... [23] Formatted ... [24] Deleted: . Formatted ... [25] Deleted: .
860	<a href="https://doi.org/10.1111/j.1462-2920.2011.02658.x">Chang, Y.-H., Cheng, T.-W., Lai, W.-J., Tsai, W.-Y., Sun, C.-H., Lin, L.-H., and Wang, P.-L.: Microbial methane cycling in a terrestrial mud volcano in eastern Taiwan, <i>Env. Microb.</i>, 14, 895–908, <a href="https://doi.org/10.1111/j.1462-2920.2011.02658.x">https://doi.org/10.1111/j.1462-2920.2011.02658.x</a>, 2012.</a>	Formatted ... [26] Deleted: ., Formatted ... [27] Deleted: .
	<a href="https://doi.org/10.1038/s41598-019-57250-9">Chen, N.-C., Yang, T. F., Hong, W.-L., Yu, T.-L., Lin, I.-T., Wang, P.-L., Lin, S., Su, C.-C., Shen, C.-C., Wang, Y., and Lin, L.-H.: Discharge of deeply rooted fluids from submarine mud volcanism in the Taiwan accretionary prism, <i>Sci. Rep.</i>, 10, 381, <a href="https://doi.org/10.1038/s41598-019-57250-9">https://doi.org/10.1038/s41598-019-57250-9</a>, 2020.</a>	Formatted ... [28] Deleted: Chao, S., Sederoff, R., and Levings, C.S.: <i>Nucleo</i> ... [29]
865	<a href="https://doi.org/10.1038/ismej.2012.61">Cheng, T.-W., Chang, Y.-H., Tang, S.-L., Tseng, C.-H., Chiang, P.-W., Chang, K.-T., Sun, C.-H., Chen, Y.-G., Kuo, H.-C., Wang, C.-H., Chu, P.-H., Song, S.-R., Wang, P.-L., and Lin, L.-H.: Metabolic stratification driven by surface and subsurface interactions in a terrestrial mud volcano, <i>ISME J.</i>, 6, 2280–2290, <a href="https://doi.org/10.1038/ismej.2012.61">https://doi.org/10.1038/ismej.2012.61</a>, 2012.</a>	Formatted ... [30] Formatted ... [31] Formatted ... [32] Deleted: .
	Cherrier, J., Bauer, J., and Druffel, E.: Utilization and turnover of labile dissolved organic matter by bacterial heterotrophs in eastern North Pacific surface waters, <i>Mar. Ecol. Prog. Ser.</i> , 139, 267–279, <a href="https://doi.org/10.3354/meps139267">https://doi.org/10.3354/meps139267</a> , 1996.	Formatted ... [33] Moved (insertion) [3]
870	<a href="https://doi.org/10.1111/j.1462-2920.2011.02658.x">Chiu, Y.-P.: Microbial community structure and methane cycling in mud volcanoes of Sicily, Italy, M.S. thesis, National Taiwan University, Taiwan, 137 pp., 2015.</a>	Formatted ... [34] Formatted ... [35] Deleted: .
	Claypool, G.E. and Kvenvolden, K.A.: Methane and other hydrocarbon gases in marine sediment, <i>Ann. Rev. Earth Planet. Sci.</i> , 11, 299–327, <a href="https://doi.org/10.1146/annurev.ea.11.050183.001503">https://doi.org/10.1146/annurev.ea.11.050183.001503</a> , 1983.	Formatted ... [36] Deleted: .
	Comte, J., Monier, A., Crevecoeur, S., Lovejoy, C., and Vincent, W.F.: Microbial biogeography of permafrost thaw ponds across the changing northern landscape, <i>Ecogeo.</i> , 39, 609–618, <a href="https://doi.org/10.1111/ecog.01667">https://doi.org/10.1111/ecog.01667</a> , 2016.	Formatted ... [37] Formatted ... [38] Deleted: Ecography,
875	Condit, R., Pitman, N., Leigh, E.G., Chave, J., Terborgh, J., Foster, R.B., Núñez, P., Aguilar, S., Valencia, R., Villa, G., Muller-Landau, H.C., Losos, E., and Hubbell, S.P.: Beta-diversity in tropical forest trees, <i>Science</i> , 295, 666–669, <a href="https://doi.org/10.1126/science.1066854">https://doi.org/10.1126/science.1066854</a> , 2002.	Formatted ... [39] Deleted: (7),
	DasSarma, S. and DasSarma, P.: Halophiles, 1–13, <a href="https://doi.org/10.1002/9780470015902.a0000394.pub4">https://doi.org/10.1002/9780470015902.a0000394.pub4</a> , 2001.	Formatted ... [40] Deleted: .
880	Dice, L.R.: Measures of the amount of ecologic association between species, <i>Ecology</i> , 26, 297–302, <a href="https://doi.org/10.2307/1932409">https://doi.org/10.2307/1932409</a> , 1945.	Formatted ... [41] Formatted ... [42] Deleted: et al
	Dimitrov, L.I.: Mud volcanoes—the most important pathway for degassing deeply buried sediments, <i>Earth-Sci. Rev.</i> , 59, 49–76, 2002.	Formatted ... [43] Deleted: (5555),
	<a href="https://doi.org/10.5194/essd-2018-108">Etiopé, G., Ciotoli, G., Schwietzke, S., and Schoell, M.: Gridded maps of geological methane emissions and their isotopic signature, <i>Earth Syst. Sci. Data Discuss.</i>, 1–29, <a href="https://doi.org/10.5194/essd-2018-108">https://doi.org/10.5194/essd-2018-108</a>, 2019.</a>	Formatted ... [44] Deleted: .
885	Ettwig, K.F., Zhu, B., Speth, D., Keltjens, J.T., Jetten, M.S.M., and Kartal, B.: Archaea catalyze iron-dependent anaerobic oxidation of methane, <i>PNAS</i> , 201609534, <a href="https://doi.org/10.1073/pnas.1609534113">https://doi.org/10.1073/pnas.1609534113</a> , 2016.	Formatted ... [45] Deleted: . In eLS, John Wiley & Sons, Ltd (Ed.),
		Formatted ... [46] Deleted: . Formatted ... [47] Deleted: 2017. Formatted ... [48] Formatted ... [49] Deleted: (3), Formatted ... [50] Deleted: . Formatted ... [51] Formatted ... [52] Deleted: doi: 10.1016/S0012-8252(02)00069-7, 2002. Formatted ... [53] Formatted ... [54] Formatted ... [55]

940 Halevy, I., Peters, S. E., and Fischer, W. W.: Sulfate **Burial Constraints** on the Phanerozoic **Sulfur Cycle**, *Science*, 337, 331–334, <https://doi.org/10.1126/science.1220224>, 2012.

Hanson, C. A., Fuhrman, J. A., Horner-Devine, M. C., and Martiny, J. B. H.: Beyond biogeographic patterns: processes shaping the microbial landscape, *Nat. Rev. Microbiol.* 10, 497, <https://doi.org/10.1038/nrmicro2795>, 2012.

945 Haroon, M. F., Hu, S., Shi, Y., Imelfort, M., Keller, J., Hugenholtz, P., **Yuan, Z.**, and **Tyson, G. W.**: Anaerobic oxidation of methane coupled to nitrate reduction in a novel archaeal lineage, *Nature*, 500, 567–570, 2013.

Hill, M. O.: Diversity and evenness: a unifying notation and its consequences, *Ecology*, 54, 427–432, 1973.

Hutchison, D. W. and Templeton, A. R.: Correlation of pairwise genetic and geographic distance measures: inferring the relative influences of gene flow and drift on the distribution of genetic variability, *Evolution*, 53, 1898–1914, 1999.

950 Inagaki, F., Nunoura, T., Nakagawa, S., Teske, A., Lever, M., Lauer, A., **Suzuki, M.**, **Takai, K.**, **Delwiche, M.**, **Colwell, F. S.**, **Nealson, K. H.**, **Horikoshi, K.**, **D'Hondt, S.**, and **Jørgensen, B. B.**: Biogeographical distribution and diversity of microbes in methane hydrate-bearing deep marine sediments on the Pacific Ocean Margin, *PNAS*, 103, 2815–2820, <https://doi.org/10.1073/pnas.0511033103>, 2006.

955 Jørgensen, S. L., Hannisdal, B., Lanzen, A., Baumberger, T., Flesland, K., Fonseca, R., **Ovreås, L.**, **Steen, I. H.**, **Thorseth, I. H.**, **Pedersen, R. B.**, and **Schleper, C.**: Correlating microbial community profiles with geochemical data in highly stratified sediments from the Arctic Mid-Ocean Ridge, *PNAS*, 109, E2846–55, <https://doi.org/10.1073/pnas.1207574109>, 2012.

Kahle, D. and Wickham, H.: ggmap: Spatial visualization with ggplot2, *R J.* 5, 144, <https://doi.org/10.32614/rj-2013-014>, 2013.

Knittel, K. and Boetius, A.: Anaerobic oxidation of methane: progress with an unknown process, *Annu. Rev. Microbiol.* 63, 311–334, <https://doi.org/10.1146/annurev.micro.61.080706.093130>, 2009.

960 **Kuever, J.**: *The Family Desulfobulbaceae*, 75–86, <https://doi.org/10.1007/978-3-642-39044-9>, 2014.

Lin, Y.-T., Tu, T.-H., Wei, C.-L., Rumble, D., Lin, L.-H., and Wang, P.-L.: Steep redox gradient and biogeochemical cycling driven by deeply sourced fluids and gases in a terrestrial mud volcano, *Fems. Microbiol. Ecol.*, 94, 3796, <https://doi.org/10.1093/femsec/fiy171>, 2018.

965 Liu, X., Li, M., Castelle, C. J., Probst, A. J., Zhou, Z., Pan, J., **Liu, Y.**, **Banfield, J. F.**, and **Gu, J.-D.**: Insights into the ecology, evolution, and metabolism of the widespread Woese archaeotal lineages, *Microbiome*, 6, 102, <https://doi.org/10.1186/s40168-018-0488-2>, 2018.

Lomolino, M. V., Riddle, B. R., and Brown, J. H.: *Biogeography* 3rd ed, edited by: **Lomolino, M. V.**, **Riddle, Brett R.**, and **Brown, J. H.**, Sinauer Associates, Inc., 2006.

970 **Martiny, J. B. H.**, **Eisen, J. A.**, **Penn, K.**, **Allison, S. D.**, and **Horner-Devine, M. C.**: Drivers of bacterial beta-diversity depend on spatial scale, *PNAS*, 108, 7850–7854, <https://doi.org/10.1073/pnas.1016308108>, 2011.

Mazzini, A. and Etiope, G.: Mud volcanism: An updated review, *Earth-Sci. Rev.* 168, 81–112, <https://doi.org/10.1016/j.earscirev.2017.03.001>, 2017.

Deleted: Grant, W.D.: Life at low water activity, Philos. T (... [59])

Deleted: burial constraints

Deleted: sulfur cycle

Formatted (... [60])

Formatted (... [61])

Formatted (... [62])

Deleted: (6092)

Formatted (... [63])

Deleted: :

Formatted (... [64])

Formatted (... [65])

Deleted: ..

Formatted (... [66])

Deleted: -506,

Deleted: :

Formatted (... [67])

Formatted (... [68])

Deleted: et al

Formatted (... [69])

Formatted (... [70])

Deleted: doi: 10.1038/nature12375,

Formatted (... [71])

Deleted: :

Formatted (... [72])

Formatted (... [73])

Deleted: doi: 10.2307/1934352,

Formatted (... [74])

Formatted (... [75])

Deleted: doi: 10.1111/j.1558-5646.1999.tb04571.x, 1999.

Formatted (... [76])

Deleted: et al

Formatted (... [77])

Deleted: ,

Formatted (... [78])

Deleted: :

Formatted (... [79])

Formatted (... [80])

Deleted: et al

Formatted (... [81])

Deleted: ,

Formatted (... [82])

Deleted: (42),

Formatted (... [83])

Deleted: -E2855,

Formatted (... [84])

Deleted: :

Formatted (... [85])

Deleted: ,

Formatted (... [86])

Deleted: ..

Formatted (... [87])

Deleted: (1),

Formatted (... [88])

Deleted: -161,

Formatted (... [89])

	McGenity, T. J.: Handbook of Hydrocarbon and Lipid Microbiology, 1939–1951, <a href="https://doi.org/10.1007/978-3-540-77587-4_142">https://doi.org/10.1007/978-3-540-77587-4_142</a> , 2010.	Deleted: Springer, Berlin, Heidelberg, doi: Formatted (... [115]) Formatted (... [116]) Deleted: 1 Formatted (... [117]) Deleted: the Deleted: Springer-Verlag, Heidelberg, Germany, 2014s Formatted (... [119]) Deleted: , and Orphan, V.J.: Single cell activity reveals (... [120]) Moved up [3]: 2015. Deleted: McGlynn Deleted: E., Chadwick, G.L., Kempes, C. Deleted: Rosenberg, E. (Eds): Formatted (... [118]) Formatted (... [123]) Formatted (... [121]) Formatted (... [122]) Deleted: prokaryotes – other major lineages Formatted (... [124]) Formatted (... [125]) Formatted (... [126]) Deleted: J., et al Formatted (... [127]) Deleted: : Formatted (... [128]) Formatted (... [129]) Deleted: et al Formatted (... [130]) Deleted: , Formatted (... [131]) Deleted: , Formatted (... [132]) Deleted: – Formatted (... [133]) Deleted: : Formatted (... [134]) Formatted (... [135]) Deleted: Ecology, Formatted (... [136]) Formatted (... [137]) Formatted (... [138]) Deleted: : Formatted (... [139]) Deleted: 1046/j.1365-2699.1999.00305.x, 1999 Formatted (... [140]) Formatted (... [141]) Deleted: : Formatted (... [142]) Deleted: : Formatted (... [143]) Formatted (... [144]) Deleted: , Formatted (... [145]) Deleted: : Formatted (... [146])
	Mellroy, S. J. and Nielsen, P. H.: The Prokaryotes, Other Major Lineages of Bacteria and The Archaea, 863–889, <a href="https://doi.org/10.1007/978-3-642-38954-2_138">https://doi.org/10.1007/978-3-642-38954-2_138</a> , 2014.	
080	Mori, J. F., Chen, L.-X., Jessen, G. L., Rudderham, S. B., McBeth, J. M., Lindsay, M. B. J., Slater, G. F., Banfield, J. F., and Warren, L. A.: Putative mixotrophic nitrifying-denitrifying Gammaproteobacteria implicated in nitrogen cycling within the ammonia/oxygen transition zone of an oil sands pit lake, <i>Front. Microbiol.</i> , 10, 2435, <a href="https://doi.org/10.3389/fmicb.2019.02435">https://doi.org/10.3389/fmicb.2019.02435</a> , 2019.	
085	Müller, A. L., Rezende, J. R. de, Hubert, C. R. J., Kjeldsen, K. U., Lagkouvardos, I., Berry, D., Jørgensen, B. B., and Loy, A.: Endospores of thermophilic bacteria as tracers of microbial dispersal by ocean currents, <i>ISME J.</i> , 8, 1153–1165, <a href="https://doi.org/10.1038/ismej.2013.225">https://doi.org/10.1038/ismej.2013.225</a> , 2014.	
	Nekola, J. C. and White, P. S.: The distance decay of similarity in biogeography and ecology, <i>J. Biogeogr.</i> , 26, 867–878, 1999.	
090	Ning, D., Deng, Y., Tiedje, J. M., and Zhou, J.: A general framework for quantitatively assessing ecological stochasticity, <i>PNAS</i> , 116, 16892–16898, <a href="https://doi.org/10.1073/pnas.1904623116">https://doi.org/10.1073/pnas.1904623116</a> , 2019.	
	Or, D., Smets, B. F., Wraith, J. M., Dechesne, A., and Friedman, S. P.: Physical constraints affecting bacterial habitats and activity in unsaturated porous media – a review, <i>Adv. Water Resour.</i> , 30, 1505–1527, <a href="https://doi.org/10.1016/j.advwatres.2006.05.025">https://doi.org/10.1016/j.advwatres.2006.05.025</a> , 2007.	
095	Orcutt, B. N., Sylvan, J. B., Knab, N. J., and Edwards, K. J.: Microbial ecology of the dark ocean above, at, and below the seafloor, <i>Microbiol. Mol. Biol. Rev.</i> , 75, 361–422, <a href="https://doi.org/10.1128/mmbr.00039-10">https://doi.org/10.1128/mmbr.00039-10</a> , 2011.	
	Orphan, V. J., Hinrichs, K.-U., Ussler, W., Paull, C. K., Taylor, L. T., Sylva, S. P., Hayes, J. M., and DeLong, E. F.: Comparative analysis of methane-oxidizing archaea and sulfate-reducing bacteria in anoxic marine sediments, <i>Appl. Environ. Microbiol.</i> , 67, 1922–1934, 2001.	
100	Paulson, J. N., Stine, O. C., Bravo, H. C., and Pop, M.: Differential abundance analysis for microbial marker-gene surveys, <i>Nat. Methods</i> , 10, 1200–2, <a href="https://doi.org/10.1038/nmeth.2658">https://doi.org/10.1038/nmeth.2658</a> , 2013.	
	Petro, C., Starnawski, P., Schramm, A., and Kjeldsen, K. U.: Microbial community assembly in marine sediments, <i>Aquat. Microb. Ecol.</i> , 79, 177–195, <a href="https://doi.org/10.3354/ame01826">https://doi.org/10.3354/ame01826</a> , 2017.	
105	Power, J. F., Carere, C. R., Lee, C. K., Wakerley, G. L. J., Evans, D. W., Button, M., White, D., Climo, M. D., Hinze, A. M., Morgan, X. C., McDonald, I. R., Cary, S. C., and Stott, M. B.: Microbial biogeography of 925 geothermal springs in New Zealand, <i>Nat. Commun.</i> , 9, 3152, <a href="https://doi.org/10.1038/s41467-018-05020-y">https://doi.org/10.1038/s41467-018-05020-y</a> , 2018.	
	Ranjard, L., Dequiedt, S., Prévost-Bouré, N. C., Thioulouse, J., Saby, N. P. A., Lelievre, M., Maron, P. A., Morin, F. E. R., Bispo, A., Jolivet, C., Arrouays, D., and Lemanceau, P.: Turnover of soil bacterial diversity driven by wide-scale environmental heterogeneity, <i>Nat. Commun.</i> , 4, 1434, <a href="https://doi.org/10.1038/ncomms2431">https://doi.org/10.1038/ncomms2431</a> , 2013.	
110	Ruff, S. E., Biddle, J. F., Teske, A. P., Knittel, K., Boetius, A., and Ramette, A.: Global dispersion and local diversification of the methane seep microbiome, <i>PNAS</i> , 112, 4015–4020, <a href="https://doi.org/10.1073/pnas.1421865112">https://doi.org/10.1073/pnas.1421865112</a> , 2015.	

	Scheller, S., Yu, H., Chadwick, G. L., McGlynn, S. E., and Orphan, V. J.: Artificial electron acceptors decouple archaeal methane oxidation from sulfate reduction, <i>Science</i> , <b>351</b> , 703–707, <a href="https://doi.org/10.1126/science.aad7154">https://doi.org/10.1126/science.aad7154</a> , 2016.	Formatted (178) Deleted: , Deleted: (6274), Deleted: :
225	Schloss, P. D., Westcott, S. L., Ryabin, T., Hall, J. R., Hartmann, M., Hollister, E. B., Lesniewski, R. A., Oakley, B. B., Parks, D. H., and Robinson, C. J.: Introducing mothur: open-source, platform-independent, community-supported software for describing and comparing microbial communities, <i>Appl. Environ. Microbiol.</i> , <b>75</b> , 7537–7541, 2009.	Formatted (179) Formatted (180) Formatted (181) Deleted: et al
	Slatkin, M.: Isolation by distance in equilibrium and non-equilibrium populations, <i>Evolution</i> , <b>47</b> , 264–279, <a href="https://doi.org/10.1111/j.1558-5646.1993.tb01215.x">https://doi.org/10.1111/j.1558-5646.1993.tb01215.x</a> , 1993.	Formatted (182) Formatted (183) Deleted: .
230	Sorokin, D. Y., Merkel, A. Y., and Muyzer, G.: <i>Bergey's Manual of Systematics of Archaea and Bacteria</i> , <b>1–6</b> , <a href="https://doi.org/10.1002/9781118960608.gbm01940">https://doi.org/10.1002/9781118960608.gbm01940</a> , 2020.	Formatted (184) Deleted: –
	Wang, P.-L., Chiu, Y.-P., Cheng, T.-W., Chang, Y.-H., Tu, W.-X., and Lin, L.-H.: Spatial variations of community structures and methane cycling across a transect of Lei-Gong-Hou mud volcanoes in eastern Taiwan, <i>Front. Microbiol.</i> , <b>5</b> , 2946, <a href="https://doi.org/10.3389/fmicb.2014.00121">https://doi.org/10.3389/fmicb.2014.00121</a> , 2014.	Formatted (185) Deleted: , doi: 10.1128/AEM.01541-09
235	Weber, L., DeForce, E., and Apprill, A.: Optimization of DNA extraction for advancing coral microbiota investigations., <i>Microbiome</i> , <b>5</b> , 18, <a href="https://doi.org/10.1186/s40168-017-0229-y">https://doi.org/10.1186/s40168-017-0229-y</a> , 2017.	Formatted (186) Formatted (187) Deleted: (1),
	Whiticar, M. J.: Carbon and hydrogen isotope systematics of bacterial formation and oxidation of methane, <i>Chem. Geol.</i> , <b>161</b> , 291–314, <a href="https://doi.org/10.1016/s0009-2541(99)00092-3">https://doi.org/10.1016/s0009-2541(99)00092-3</a> , 1999.	Formatted (188) Deleted: :
240	Yamada, T. and Sekiguchi, Y.: Cultivation of <i>Uncultured Chloroflexi</i> Subphyla: Significance and Ecophysiology of Formerly <i>Uncultured Chloroflexi</i> “Subphylum I” with Natural and Biotechnological Relevance, <i>Microbes Environment</i> , <b>24</b> , 205–216, <a href="https://doi.org/10.1264/jsme2.me09151s">https://doi.org/10.1264/jsme2.me09151s</a> , 2009.	Formatted (189) Formatted (190) Deleted: (Eds.):
	Yao, W. and Millero, F. J.: Oxidation of hydrogen sulfide by hydrous Fe(III) oxides in seawater, <i>Mar. Chem.</i> , <b>52</b> , 1–16, <a href="https://doi.org/10.1016/0304-4203(95)00072-0">https://doi.org/10.1016/0304-4203(95)00072-0</a> , 1996.	Formatted (191) Deleted: Hoboken, New Jersey, USA, 2015
245	Zheng, G., Xu, S., Liang, M., Dermatas, D., and Xu, X.: Transformations of organic carbon and its impact on lead weathering in shooting range soils, <i>Environ. Earth Sci.</i> , <b>64</b> , 2241–2246, <a href="https://doi.org/10.1007/s12665-011-1052-6">https://doi.org/10.1007/s12665-011-1052-6</a> , 2011.	Formatted (192) Deleted: Starnawski
	Zinger, L., Boetius, A., and Ramette, A.: Bacterial taxa-area and distance-decay relationships in marine environments, <i>Mol. Ecol.</i> , <b>23</b> , 954–964, <a href="https://doi.org/10.1111/mec.12640">https://doi.org/10.1111/mec.12640</a> , 2014.	Formatted (193) Deleted: , Bataillon
		Formatted (194) Deleted: , Ettema, T.J.G., Joehum, L.M., Schreiber, L., Chen,
		Formatted (195) Deleted: et al.: Microbial
		Formatted (196) Deleted: assembly and evolution in subsurface sediment (... [197])
		Formatted (198) Deleted: Thandrup, B.: Anaerobic methanotrophic archaea (... [199])
		Formatted (200) Deleted: 8, 619,
		Formatted (201) Deleted: :
		Formatted (202) Deleted: 2017.00619, 2017
		Formatted (203) Formatted (204) Formatted (205) Formatted (206) Deleted: :
		Formatted (207) Deleted: S0009
		Formatted (208) Deleted: uncultured chloroflexi subphyla: significance
		Formatted (209) Deleted: ecophysiology
		Formatted (210)

**Page 5: [1] Formatted** Tzu-Hsuan Tu 10/17/21 10:44:00 PM

English (US)

**Page 5: [1] Formatted** Tzu-Hsuan Tu 10/17/21 10:44:00 PM

English (US)

**Page 5: [2] Formatted** Tzu-Hsuan Tu 10/17/21 10:44:00 PM

English (US)

**Page 5: [2] Formatted** Tzu-Hsuan Tu 10/17/21 10:44:00 PM

English (US)

**Page 5: [3] Formatted** Tzu-Hsuan Tu 10/17/21 10:44:00 PM

English (US)

**Page 5: [3] Formatted** Tzu-Hsuan Tu 10/17/21 10:44:00 PM

English (US)

**Page 5: [4] Formatted** Tzu-Hsuan Tu 10/17/21 10:44:00 PM

English (US)

**Page 5: [4] Formatted** Tzu-Hsuan Tu 10/17/21 10:44:00 PM

English (US)

**Page 5: [4] Formatted** Tzu-Hsuan Tu 10/17/21 10:44:00 PM

English (US)

**Page 5: [5] Formatted** Tzu-Hsuan Tu 10/17/21 10:44:00 PM

English (US)

**Page 5: [5] Formatted** Tzu-Hsuan Tu 10/17/21 10:44:00 PM

English (US)

**Page 5: [5] Formatted** Tzu-Hsuan Tu 10/17/21 10:44:00 PM

English (US)

**Page 5: [6] Formatted** Tzu-Hsuan Tu 10/17/21 10:44:00 PM

English (US)

**Page 5: [6] Formatted** Tzu-Hsuan Tu 10/17/21 10:44:00 PM

English (US)

**Page 5: [6] Formatted** Tzu-Hsuan Tu 10/17/21 10:44:00 PM

English (US)

**Page 5: [6] Formatted** Tzu-Hsuan Tu 10/17/21 10:44:00 PM

English (US)

▲ **Page 5: [7] Formatted** Tzu-Hsuan Tu 10/17/21 10:44:00 PM

English (US)

▲ **Page 5: [7] Formatted** Tzu-Hsuan Tu 10/17/21 10:44:00 PM

English (US)

▲ **Page 5: [7] Formatted** Tzu-Hsuan Tu 10/17/21 10:44:00 PM

English (US)

▲ **Page 12: [8] Formatted** Tzu-Hsuan Tu 10/17/21 10:44:00 PM

English (US)

▲ **Page 12: [8] Formatted** Tzu-Hsuan Tu 10/17/21 10:44:00 PM

English (US)

▲ **Page 12: [9] Deleted** Tzu-Hsuan Tu 10/17/21 10:44:00 PM

▼  
▲ **Page 12: [9] Deleted** Tzu-Hsuan Tu 10/17/21 10:44:00 PM

▼  
▲ **Page 12: [10] Deleted** Tzu-Hsuan Tu 10/17/21 10:44:00 PM

▼  
▲ **Page 12: [10] Deleted** Tzu-Hsuan Tu 10/17/21 10:44:00 PM

▼  
▲ **Page 12: [10] Deleted** Tzu-Hsuan Tu 10/17/21 10:44:00 PM

▼  
▲ **Page 12: [10] Deleted** Tzu-Hsuan Tu 10/17/21 10:44:00 PM

▼  
▲ **Page 12: [10] Deleted** Tzu-Hsuan Tu 10/17/21 10:44:00 PM

▼  
▲ **Page 12: [10] Deleted** Tzu-Hsuan Tu 10/17/21 10:44:00 PM

▼  
▲ **Page 12: [10] Deleted** Tzu-Hsuan Tu 10/17/21 10:44:00 PM

▼  
▲ **Page 12: [11] Deleted** Tzu-Hsuan Tu 10/17/21 10:44:00 PM

▼  
▲ **Page 12: [11] Deleted** Tzu-Hsuan Tu 10/17/21 10:44:00 PM

▼  
▲  
**Page 12: [11] Deleted** Tzu-Hsuan Tu 10/17/21 10:44:00 PM

▼  
▲  
**Page 12: [12] Deleted** Tzu-Hsuan Tu 10/17/21 10:44:00 PM

▼  
▲  
**Page 12: [12] Deleted** Tzu-Hsuan Tu 10/17/21 10:44:00 PM

▼  
▲  
**Page 12: [13] Deleted** Tzu-Hsuan Tu 10/17/21 10:44:00 PM

▼  
▲  
**Page 12: [13] Deleted** Tzu-Hsuan Tu 10/17/21 10:44:00 PM

▼  
▲  
**Page 12: [13] Deleted** Tzu-Hsuan Tu 10/17/21 10:44:00 PM

▼  
▲  
**Page 12: [13] Deleted** Tzu-Hsuan Tu 10/17/21 10:44:00 PM

▼  
▲  
**Page 12: [13] Deleted** Tzu-Hsuan Tu 10/17/21 10:44:00 PM

▼  
▲  
**Page 17: [14] Formatted** Tzu-Hsuan Tu 10/17/21 10:44:00 PM

Font: 10 pt, Font color: Black, English (UK)

▼  
▲  
**Page 17: [14] Formatted** Tzu-Hsuan Tu 10/17/21 10:44:00 PM

Font: 10 pt, Font color: Black, English (UK)

▼  
▲  
**Page 17: [14] Formatted** Tzu-Hsuan Tu 10/17/21 10:44:00 PM

Font: 10 pt, Font color: Black, English (UK)

▼  
▲  
**Page 17: [14] Formatted** Tzu-Hsuan Tu 10/17/21 10:44:00 PM

Font: 10 pt, Font color: Black, English (UK)

▼  
▲  
**Page 17: [14] Formatted** Tzu-Hsuan Tu 10/17/21 10:44:00 PM

Font: 10 pt, Font color: Black, English (UK)

▼  
▲  
**Page 17: [14] Formatted** Tzu-Hsuan Tu 10/17/21 10:44:00 PM

Font: 10 pt, Font color: Black, English (UK)

▼  
▲  
**Page 17: [14] Formatted** Tzu-Hsuan Tu 10/17/21 10:44:00 PM

Font: 10 pt, Font color: Black, English (UK)



**Page 17: [15] Formatted Tzu-Hsuan Tu 10/17/21 10:44:00 PM**

Font: 10 pt, Font color: Black, English (UK)

**Page 17: [15] Formatted Tzu-Hsuan Tu 10/17/21 10:44:00 PM**

Font: 10 pt, Font color: Black, English (UK)

**Page 17: [15] Formatted Tzu-Hsuan Tu 10/17/21 10:44:00 PM**

Font: 10 pt, Font color: Black, English (UK)

**Page 17: [15] Formatted Tzu-Hsuan Tu 10/17/21 10:44:00 PM**

Font: 10 pt, Font color: Black, English (UK)

**Page 17: [15] Formatted Tzu-Hsuan Tu 10/17/21 10:44:00 PM**

Font: 10 pt, Font color: Black, English (UK)

**Page 17: [15] Formatted Tzu-Hsuan Tu 10/17/21 10:44:00 PM**

Font: 10 pt, Font color: Black, English (UK)

**Page 17: [16] Formatted Tzu-Hsuan Tu 10/17/21 10:44:00 PM**

Font: 10 pt, Font color: Black, English (UK)

**Page 17: [16] Formatted Tzu-Hsuan Tu 10/17/21 10:44:00 PM**

Font: 10 pt, Font color: Black, English (UK)

**Page 17: [17] Formatted Tzu-Hsuan Tu 10/17/21 10:44:00 PM**

Font: 10 pt, Font color: Black, English (UK)

**Page 17: [17] Formatted Tzu-Hsuan Tu 10/17/21 10:44:00 PM**

Font: 10 pt, Font color: Black, English (UK)

**Page 17: [18] Formatted Tzu-Hsuan Tu 10/17/21 10:44:00 PM**

Font: 10 pt, Font color: Black, English (UK)

**Page 17: [18] Formatted Tzu-Hsuan Tu 10/17/21 10:44:00 PM**

Font: 10 pt, Font color: Black, English (UK)

**Page 17: [18] Formatted Tzu-Hsuan Tu 10/17/21 10:44:00 PM**

Font: 10 pt, Font color: Black, English (UK)

**Page 17: [18] Formatted Tzu-Hsuan Tu 10/17/21 10:44:00 PM**

Font: 10 pt, Font color: Black, English (UK)

**Page 17: [18] Formatted Tzu-Hsuan Tu 10/17/21 10:44:00 PM**

Font: 10 pt, Font color: Black, English (UK)

**Page 17: [18] Formatted Tzu-Hsuan Tu 10/17/21 10:44:00 PM**

Font: 10 pt, Font color: Black, English (UK)

▲  
**Page 17: [18] Formatted Tzu-Hsuan Tu 10/17/21 10:44:00 PM**

Font: 10 pt, Font color: Black, English (UK)

▲  
**Page 17: [18] Formatted Tzu-Hsuan Tu 10/17/21 10:44:00 PM**

Font: 10 pt, Font color: Black, English (UK)

▲  
**Page 17: [18] Formatted Tzu-Hsuan Tu 10/17/21 10:44:00 PM**

Font: 10 pt, Font color: Black, English (UK)

▲  
**Page 17: [18] Formatted Tzu-Hsuan Tu 10/17/21 10:44:00 PM**

Font: 10 pt, Font color: Black, English (UK)

▲  
**Page 17: [18] Formatted Tzu-Hsuan Tu 10/17/21 10:44:00 PM**

Font: 10 pt, Font color: Black, English (UK)

▲  
**Page 17: [18] Formatted Tzu-Hsuan Tu 10/17/21 10:44:00 PM**

Font: 10 pt, Font color: Black, English (UK)

▲  
**Page 17: [19] Formatted Tzu-Hsuan Tu 10/17/21 10:44:00 PM**

Font: 10 pt, Font color: Black, English (UK)

▲  
**Page 17: [19] Formatted Tzu-Hsuan Tu 10/17/21 10:44:00 PM**

Font: 10 pt, Font color: Black, English (UK)

▲  
**Page 17: [20] Formatted Tzu-Hsuan Tu 10/17/21 10:44:00 PM**

Font: 10 pt, Font color: Black, English (UK)

▲  
**Page 17: [20] Formatted Tzu-Hsuan Tu 10/17/21 10:44:00 PM**

Font: 10 pt, Font color: Black, English (UK)

▲  
**Page 17: [20] Formatted Tzu-Hsuan Tu 10/17/21 10:44:00 PM**

Font: 10 pt, Font color: Black, English (UK)

▲  
**Page 17: [21] Formatted Tzu-Hsuan Tu 10/17/21 10:44:00 PM**

Font: 10 pt, Font color: Black, English (UK)

▲  
**Page 17: [21] Formatted Tzu-Hsuan Tu 10/17/21 10:44:00 PM**

Font: 10 pt, Font color: Black, English (UK)

▲  
**Page 18: [22] Formatted Tzu-Hsuan Tu 10/17/21 10:44:00 PM**

Font: 10 pt, Font color: Black, English (UK)

▲  
**Page 18: [22] Formatted Tzu-Hsuan Tu 10/17/21 10:44:00 PM**

Font: 10 pt, Font color: Black, English (UK)

▲  
**Page 18: [23] Formatted Tzu-Hsuan Tu 10/17/21 10:44:00 PM**

Font: 10 pt, Font color: Black, English (UK)

Font: 10 pt, Font color: Black, English (UK)

▲  
**Page 18: [25] Formatted Tzu-Hsuan Tu 10/17/21 10:44:00 PM**

Font: 10 pt, Font color: Black, English (UK)

▲  
**Page 18: [26] Formatted Tzu-Hsuan Tu 10/17/21 10:44:00 PM**

Font: 10 pt, Font color: Black, English (UK)

▲  
**Page 18: [27] Formatted Tzu-Hsuan Tu 10/17/21 10:44:00 PM**

Font: 10 pt, Font color: Black, English (UK)

▲  
**Page 18: [27] Formatted Tzu-Hsuan Tu 10/17/21 10:44:00 PM**

Font: 10 pt, Font color: Black, English (UK)

▲  
**Page 18: [28] Formatted Tzu-Hsuan Tu 10/17/21 10:44:00 PM**

Font: 10 pt, Font color: Black, English (UK)

▲  
**Page 18: [29] Deleted Tzu-Hsuan Tu 10/17/21 10:44:00 PM**

▼  
**Page 18: [30] Formatted Tzu-Hsuan Tu 10/17/21 10:44:00 PM**

Font: 10 pt, Font color: Black, English (UK)

▲  
**Page 18: [31] Formatted Tzu-Hsuan Tu 10/17/21 10:44:00 PM**

csl-entry

▲  
**Page 18: [32] Formatted Tzu-Hsuan Tu 10/17/21 10:44:00 PM**

Font: 10 pt, Font color: Black

▲  
**Page 18: [32] Formatted Tzu-Hsuan Tu 10/17/21 10:44:00 PM**

Font: 10 pt, Font color: Black

▲  
**Page 18: [32] Formatted Tzu-Hsuan Tu 10/17/21 10:44:00 PM**

Font: 10 pt, Font color: Black

▲  
**Page 18: [32] Formatted Tzu-Hsuan Tu 10/17/21 10:44:00 PM**

Font: 10 pt, Font color: Black

▲  
**Page 18: [32] Formatted Tzu-Hsuan Tu 10/17/21 10:44:00 PM**

Font: 10 pt, Font color: Black

▲  
**Page 18: [32] Formatted Tzu-Hsuan Tu 10/17/21 10:44:00 PM**

Font: 10 pt, Font color: Black

▲  
**Page 18: [32] Formatted Tzu-Hsuan Tu 10/17/21 10:44:00 PM**

Font: 10 pt, Font color: Black

▲  
**Page 18: [32] Formatted Tzu-Hsuan Tu 10/17/21 10:44:00 PM**

Font: 10 pt, Font color: Black

Font: 10 pt, Font color: Black

▲  
**Page 18: [33] Formatted Tzu-Hsuan Tu 10/17/21 10:44:00 PM**

Font: 10 pt, Font color: Black, English (UK)

▲  
**Page 18: [34] Formatted Tzu-Hsuan Tu 10/17/21 10:44:00 PM**

Font: 10 pt, Font color: Black, English (UK)

▲  
**Page 18: [35] Formatted Tzu-Hsuan Tu 10/17/21 10:44:00 PM**

Font: 10 pt, Font color: Black, English (UK)

▲  
**Page 18: [35] Formatted Tzu-Hsuan Tu 10/17/21 10:44:00 PM**

Font: 10 pt, Font color: Black, English (UK)

▲  
**Page 18: [36] Formatted Tzu-Hsuan Tu 10/17/21 10:44:00 PM**

Font: 10 pt, Font color: Black, English (UK)

▲  
**Page 18: [36] Formatted Tzu-Hsuan Tu 10/17/21 10:44:00 PM**

Font: 10 pt, Font color: Black, English (UK)

▲  
**Page 18: [37] Formatted Tzu-Hsuan Tu 10/17/21 10:44:00 PM**

Font: 10 pt, Font color: Black, English (UK)

▲  
**Page 18: [38] Formatted Tzu-Hsuan Tu 10/17/21 10:44:00 PM**

Font: 10 pt, Font color: Black, English (UK)

▲  
**Page 18: [39] Formatted Tzu-Hsuan Tu 10/17/21 10:44:00 PM**

Font: 10 pt, Font color: Black

▲  
**Page 18: [39] Formatted Tzu-Hsuan Tu 10/17/21 10:44:00 PM**

Font: 10 pt, Font color: Black

▲  
**Page 18: [40] Formatted Tzu-Hsuan Tu 10/17/21 10:44:00 PM**

Font: 10 pt, Font color: Black, English (UK)

▲  
**Page 18: [40] Formatted Tzu-Hsuan Tu 10/17/21 10:44:00 PM**

Font: 10 pt, Font color: Black, English (UK)

▲  
**Page 18: [41] Formatted Tzu-Hsuan Tu 10/17/21 10:44:00 PM**

Font: 10 pt, Font color: Black, English (UK)

▲  
**Page 18: [42] Formatted Tzu-Hsuan Tu 10/17/21 10:44:00 PM**

Font: 10 pt, Font color: Black, English (UK)

▲  
**Page 18: [42] Formatted Tzu-Hsuan Tu 10/17/21 10:44:00 PM**

Font: 10 pt, Font color: Black, English (UK)

▲

**Page 18: [43] Formatted Tzu-Hsuan Tu 10/17/21 10:44:00 PM**

Font: 10 pt, Font color: Black, English (UK)

**Page 18: [43] Formatted Tzu-Hsuan Tu 10/17/21 10:44:00 PM**

Font: 10 pt, Font color: Black, English (UK)

**Page 18: [44] Formatted Tzu-Hsuan Tu 10/17/21 10:44:00 PM**

Font: 10 pt, Font color: Black, English (UK)

**Page 18: [44] Formatted Tzu-Hsuan Tu 10/17/21 10:44:00 PM**

Font: 10 pt, Font color: Black, English (UK)

**Page 18: [45] Formatted Tzu-Hsuan Tu 10/17/21 10:44:00 PM**

Font: 10 pt, Font color: Black, English (UK)

**Page 18: [46] Formatted Tzu-Hsuan Tu 10/17/21 10:44:00 PM**

Font: 10 pt, Font color: Black, English (UK)

**Page 18: [47] Formatted Tzu-Hsuan Tu 10/17/21 10:44:00 PM**

Font: 10 pt, Font color: Black, English (UK)

**Page 18: [48] Formatted Tzu-Hsuan Tu 10/17/21 10:44:00 PM**

Font: 10 pt, Font color: Black, English (UK)

**Page 18: [49] Formatted Tzu-Hsuan Tu 10/17/21 10:44:00 PM**

Font: 10 pt, Font color: Black, English (UK)

**Page 18: [50] Formatted Tzu-Hsuan Tu 10/17/21 10:44:00 PM**

Font: 10 pt, Font color: Black, English (UK)

**Page 18: [50] Formatted Tzu-Hsuan Tu 10/17/21 10:44:00 PM**

Font: 10 pt, Font color: Black, English (UK)

**Page 18: [51] Formatted Tzu-Hsuan Tu 10/17/21 10:44:00 PM**

Font: 10 pt, Font color: Black, English (UK)

**Page 18: [52] Formatted Tzu-Hsuan Tu 10/17/21 10:44:00 PM**

Font: 10 pt, Font color: Black, English (UK)

**Page 18: [53] Formatted Tzu-Hsuan Tu 10/17/21 10:44:00 PM**

Font: 10 pt, Font color: Black, English (UK)

**Page 18: [54] Formatted Tzu-Hsuan Tu 10/17/21 10:44:00 PM**

Font: 10 pt, Font color: Black, English (UK)

**Page 18: [55] Formatted Tzu-Hsuan Tu 10/17/21 10:44:00 PM**

csl-entry

▲  
**Page 18: [56] Formatted Tzu-Hsuan Tu 10/17/21 10:44:00 PM**

Font: 10 pt, Font color: Black, English (UK)

▲  
**Page 18: [56] Formatted Tzu-Hsuan Tu 10/17/21 10:44:00 PM**

Font: 10 pt, Font color: Black, English (UK)

▲  
**Page 18: [56] Formatted Tzu-Hsuan Tu 10/17/21 10:44:00 PM**

Font: 10 pt, Font color: Black, English (UK)

▲  
**Page 18: [57] Formatted Tzu-Hsuan Tu 10/17/21 10:44:00 PM**

Font: 10 pt, Font color: Black, English (UK)

▲  
**Page 18: [58] Formatted Tzu-Hsuan Tu 10/17/21 10:44:00 PM**

Font: 10 pt, Font color: Black, English (UK)

▲  
**Page 19: [59] Deleted Tzu-Hsuan Tu 10/17/21 10:44:00 PM**

▼  
**Page 19: [60] Formatted Tzu-Hsuan Tu 10/17/21 10:44:00 PM**

Font: 10 pt, Font color: Black, English (UK)

▲  
**Page 19: [60] Formatted Tzu-Hsuan Tu 10/17/21 10:44:00 PM**

Font: 10 pt, Font color: Black, English (UK)

▲  
**Page 19: [60] Formatted Tzu-Hsuan Tu 10/17/21 10:44:00 PM**

Font: 10 pt, Font color: Black, English (UK)

▲  
**Page 19: [61] Formatted Tzu-Hsuan Tu 10/17/21 10:44:00 PM**

Font: 10 pt, Font color: Black, English (UK)

▲  
**Page 19: [62] Formatted Tzu-Hsuan Tu 10/17/21 10:44:00 PM**

Font: 10 pt, Font color: Black, English (UK)

▲  
**Page 19: [63] Formatted Tzu-Hsuan Tu 10/17/21 10:44:00 PM**

Font: 10 pt, Font color: Black, English (UK)

▲  
**Page 19: [63] Formatted Tzu-Hsuan Tu 10/17/21 10:44:00 PM**

Font: 10 pt, Font color: Black, English (UK)

▲  
**Page 19: [64] Formatted Tzu-Hsuan Tu 10/17/21 10:44:00 PM**

Font: 10 pt, Font color: Black, English (UK)

▲  
**Page 19: [65] Formatted Tzu-Hsuan Tu 10/17/21 10:44:00 PM**

Font: 10 pt, Font color: Black, English (UK)

▲  
**Page 19: [65] Formatted Tzu-Hsuan Tu 10/17/21 10:44:00 PM**

Font: 10 pt, Font color: Black, English (UK)

▲

**Page 19: [65] Formatted Tzu-Hsuan Tu 10/17/21 10:44:00 PM**

Font: 10 pt, Font color: Black, English (UK)

**Page 19: [65] Formatted Tzu-Hsuan Tu 10/17/21 10:44:00 PM**

Font: 10 pt, Font color: Black, English (UK)

**Page 19: [66] Formatted Tzu-Hsuan Tu 10/17/21 10:44:00 PM**

Font: 10 pt, Font color: Black, English (UK)

**Page 19: [67] Formatted Tzu-Hsuan Tu 10/17/21 10:44:00 PM**

Font: 10 pt, Font color: Black, English (UK)

**Page 19: [68] Formatted Tzu-Hsuan Tu 10/17/21 10:44:00 PM**

Font: 10 pt, Font color: Black, English (UK)

**Page 19: [69] Formatted Tzu-Hsuan Tu 10/17/21 10:44:00 PM**

Font: 10 pt, Font color: Black, English (UK)

**Page 19: [70] Formatted Tzu-Hsuan Tu 10/17/21 10:44:00 PM**

Font: 10 pt, Font color: Black, English (UK)

**Page 19: [70] Formatted Tzu-Hsuan Tu 10/17/21 10:44:00 PM**

Font: 10 pt, Font color: Black, English (UK)

**Page 19: [70] Formatted Tzu-Hsuan Tu 10/17/21 10:44:00 PM**

Font: 10 pt, Font color: Black, English (UK)

**Page 19: [71] Formatted Tzu-Hsuan Tu 10/17/21 10:44:00 PM**

Font: 10 pt, Font color: Black, English (UK)

**Page 19: [72] Formatted Tzu-Hsuan Tu 10/17/21 10:44:00 PM**

Font: 10 pt, Font color: Black, English (UK)

**Page 19: [73] Formatted Tzu-Hsuan Tu 10/17/21 10:44:00 PM**

Font: 10 pt, Font color: Black, English (UK)

**Page 19: [73] Formatted Tzu-Hsuan Tu 10/17/21 10:44:00 PM**

Font: 10 pt, Font color: Black, English (UK)

**Page 19: [73] Formatted Tzu-Hsuan Tu 10/17/21 10:44:00 PM**

Font: 10 pt, Font color: Black, English (UK)

**Page 19: [74] Formatted Tzu-Hsuan Tu 10/17/21 10:44:00 PM**

Font: 10 pt, Font color: Black, English (UK)

**Page 19: [75] Formatted Tzu-Hsuan Tu 10/17/21 10:44:00 PM**

Font: 10 pt, Font color: Black, English (UK)

▲  
**Page 19: [75] Formatted Tzu-Hsuan Tu 10/17/21 10:44:00 PM**

Font: 10 pt, Font color: Black, English (UK)

▲  
**Page 19: [75] Formatted Tzu-Hsuan Tu 10/17/21 10:44:00 PM**

Font: 10 pt, Font color: Black, English (UK)

▲  
**Page 19: [76] Formatted Tzu-Hsuan Tu 10/17/21 10:44:00 PM**

Font: 10 pt, Font color: Black, English (UK)

▲  
**Page 19: [77] Formatted Tzu-Hsuan Tu 10/17/21 10:44:00 PM**

Font: 10 pt, Font color: Black, English (UK)

▲  
**Page 19: [78] Formatted Tzu-Hsuan Tu 10/17/21 10:44:00 PM**

Font: 10 pt, Font color: Black, English (UK)

▲  
**Page 19: [78] Formatted Tzu-Hsuan Tu 10/17/21 10:44:00 PM**

Font: 10 pt, Font color: Black, English (UK)

▲  
**Page 19: [79] Formatted Tzu-Hsuan Tu 10/17/21 10:44:00 PM**

Font: 10 pt, Font color: Black, English (UK)

▲  
**Page 19: [80] Formatted Tzu-Hsuan Tu 10/17/21 10:44:00 PM**

Font: 10 pt, Font color: Black, English (UK)

▲  
**Page 19: [81] Formatted Tzu-Hsuan Tu 10/17/21 10:44:00 PM**

Font: 10 pt, Font color: Black, English (UK)

▲  
**Page 19: [82] Formatted Tzu-Hsuan Tu 10/17/21 10:44:00 PM**

Font: 10 pt, Font color: Black, English (UK)

▲  
**Page 19: [83] Formatted Tzu-Hsuan Tu 10/17/21 10:44:00 PM**

Font: 10 pt, Font color: Black, English (UK)

▲  
**Page 19: [84] Formatted Tzu-Hsuan Tu 10/17/21 10:44:00 PM**

Font: 10 pt, Font color: Black, English (UK)

▲  
**Page 19: [85] Formatted Tzu-Hsuan Tu 10/17/21 10:44:00 PM**

Font: 10 pt, Font color: Black, English (UK)

▲  
**Page 19: [86] Formatted Tzu-Hsuan Tu 10/17/21 10:44:00 PM**

Font: 10 pt, Font color: Black, English (UK)

▲  
**Page 19: [87] Formatted Tzu-Hsuan Tu 10/17/21 10:44:00 PM**

Font: 10 pt, Font color: Black, English (UK)

▲  
**Page 19: [88] Formatted Tzu-Hsuan Tu 10/17/21 10:44:00 PM**

Font: 10 pt, Font color: Black, English (UK)



Font: 10 pt, Font color: Black, English (UK)

▲  
**Page 19: [90] Formatted Tzu-Hsuan Tu 10/17/21 10:44:00 PM**

Font: 10 pt, Font color: Black, English (UK)

▲  
**Page 19: [91] Formatted Tzu-Hsuan Tu 10/17/21 10:44:00 PM**

Font: 10 pt, Font color: Black, English (UK)

▲  
**Page 19: [92] Formatted Tzu-Hsuan Tu 10/17/21 10:44:00 PM**

Font: 10 pt, Font color: Black, English (UK)

▲  
**Page 19: [92] Formatted Tzu-Hsuan Tu 10/17/21 10:44:00 PM**

Font: 10 pt, Font color: Black, English (UK)

▲  
**Page 19: [92] Formatted Tzu-Hsuan Tu 10/17/21 10:44:00 PM**

Font: 10 pt, Font color: Black, English (UK)

▲  
**Page 19: [92] Formatted Tzu-Hsuan Tu 10/17/21 10:44:00 PM**

Font: 10 pt, Font color: Black, English (UK)

▲  
**Page 19: [93] Formatted Tzu-Hsuan Tu 10/17/21 10:44:00 PM**

Font: 10 pt, Font color: Black, English (UK)

▲  
**Page 19: [94] Deleted Tzu-Hsuan Tu 10/17/21 10:44:00 PM**

▼  
**Page 19: [95] Formatted Tzu-Hsuan Tu 10/17/21 10:44:00 PM**

Font: 10 pt, Font color: Black, English (UK)

▲  
**Page 19: [96] Formatted Tzu-Hsuan Tu 10/17/21 10:44:00 PM**

csl-entry

▲  
**Page 19: [97] Formatted Tzu-Hsuan Tu 10/17/21 10:44:00 PM**

Font: 10 pt, Font color: Black, English (UK)

▲  
**Page 19: [98] Formatted Tzu-Hsuan Tu 10/17/21 10:44:00 PM**

Font: 10 pt, Font color: Black, English (UK)

▲  
**Page 19: [99] Formatted Tzu-Hsuan Tu 10/17/21 10:44:00 PM**

Font: 10 pt, Font color: Black, English (UK)

▲  
**Page 19: [100] Formatted Tzu-Hsuan Tu 10/17/21 10:44:00 PM**

Font: 10 pt, Font color: Black, English (UK)

▲  
**Page 19: [100] Formatted Tzu-Hsuan Tu 10/17/21 10:44:00 PM**

Font: 10 pt, Font color: Black, English (UK)

▲  
**Page 19: [101] Formatted Tzu-Hsuan Tu 10/17/21 10:44:00 PM**

Font: 10 pt, Font color: Black, English (UK)

Font: 10 pt, Font color: Black, English (UK)

▲  
**Page 19: [103] Formatted**      **Tzu-Hsuan Tu**      **10/17/21 10:44:00 PM**

Font: 10 pt, Font color: Black, English (UK)

▲  
**Page 19: [104] Formatted**      **Tzu-Hsuan Tu**      **10/17/21 10:44:00 PM**

Font: 10 pt, Font color: Black, English (UK)

▲  
**Page 19: [104] Formatted**      **Tzu-Hsuan Tu**      **10/17/21 10:44:00 PM**

Font: 10 pt, Font color: Black, English (UK)

▲  
**Page 19: [104] Formatted**      **Tzu-Hsuan Tu**      **10/17/21 10:44:00 PM**

Font: 10 pt, Font color: Black, English (UK)

▲  
**Page 19: [105] Formatted**      **Tzu-Hsuan Tu**      **10/17/21 10:44:00 PM**

Font: 10 pt, Font color: Black, English (UK)

▲  
**Page 19: [106] Deleted**      **Tzu-Hsuan Tu**      **10/17/21 10:44:00 PM**

▼  
▲  
**Page 19: [107] Formatted**      **Tzu-Hsuan Tu**      **10/17/21 10:44:00 PM**

Font: 10 pt, Font color: Black, English (UK)

▲  
**Page 19: [107] Formatted**      **Tzu-Hsuan Tu**      **10/17/21 10:44:00 PM**

Font: 10 pt, Font color: Black, English (UK)

▲  
**Page 19: [108] Formatted**      **Tzu-Hsuan Tu**      **10/17/21 10:44:00 PM**

Font: 10 pt, Font color: Black, English (UK)

▲  
**Page 19: [108] Formatted**      **Tzu-Hsuan Tu**      **10/17/21 10:44:00 PM**

Font: 10 pt, Font color: Black, English (UK)

▲  
**Page 19: [108] Formatted**      **Tzu-Hsuan Tu**      **10/17/21 10:44:00 PM**

Font: 10 pt, Font color: Black, English (UK)

▲  
**Page 19: [108] Formatted**      **Tzu-Hsuan Tu**      **10/17/21 10:44:00 PM**

Font: 10 pt, Font color: Black, English (UK)

▲  
**Page 19: [108] Formatted**      **Tzu-Hsuan Tu**      **10/17/21 10:44:00 PM**

Font: 10 pt, Font color: Black, English (UK)

▲  
**Page 19: [108] Formatted**      **Tzu-Hsuan Tu**      **10/17/21 10:44:00 PM**

Font: 10 pt, Font color: Black, English (UK)

▲  
**Page 19: [108] Formatted**      **Tzu-Hsuan Tu**      **10/17/21 10:44:00 PM**

**Page 19: [109] Formatted** Tzu-Hsuan Tu 10/17/21 10:44:00 PM

Font: 10 pt, Font color: Black, English (UK)

**Page 19: [110] Formatted** Tzu-Hsuan Tu 10/17/21 10:44:00 PM

Font: 10 pt, Font color: Black, English (UK)

**Page 19: [110] Formatted** Tzu-Hsuan Tu 10/17/21 10:44:00 PM

Font: 10 pt, Font color: Black, English (UK)

**Page 19: [111] Formatted** Tzu-Hsuan Tu 10/17/21 10:44:00 PM

Font: 10 pt, Font color: Black, English (UK)

**Page 19: [112] Formatted** Tzu-Hsuan Tu 10/17/21 10:44:00 PM

Font: 10 pt, Font color: Black, English (UK)

**Page 19: [113] Formatted** Tzu-Hsuan Tu 10/17/21 10:44:00 PM

Font: 10 pt, Font color: Black, English (UK)

**Page 19: [113] Formatted** Tzu-Hsuan Tu 10/17/21 10:44:00 PM

Font: 10 pt, Font color: Black, English (UK)

**Page 19: [114] Formatted** Tzu-Hsuan Tu 10/17/21 10:44:00 PM

Font: 10 pt, Font color: Black, English (UK)

**Page 20: [115] Formatted** Tzu-Hsuan Tu 10/17/21 10:44:00 PM

Font: 10 pt, Font color: Black, English (UK)

**Page 20: [116] Formatted** Tzu-Hsuan Tu 10/17/21 10:44:00 PM

Font: 10 pt, Font color: Black, English (UK)

**Page 20: [117] Formatted** Tzu-Hsuan Tu 10/17/21 10:44:00 PM

Font: 10 pt, Font color: Black, English (UK)

**Page 20: [118] Formatted** Tzu-Hsuan Tu 10/17/21 10:44:00 PM

Font: 10 pt, Font color: Black, English (UK)

**Page 20: [119] Formatted** Tzu-Hsuan Tu 10/17/21 10:44:00 PM

Font: 10 pt, Font color: Black, English (UK)

**Page 20: [120] Deleted** Tzu-Hsuan Tu 10/17/21 10:44:00 PM

**Page 20: [121] Formatted** Tzu-Hsuan Tu 10/17/21 10:44:00 PM

Font: 10 pt, Font color: Black, English (UK)

▲  
**Page 20: [123] Formatted**      **Tzu-Hsuan Tu**      **10/17/21 10:44:00 PM**

Font: 10 pt, Font color: Black, English (UK)

▲  
**Page 20: [124] Formatted**      **Tzu-Hsuan Tu**      **10/17/21 10:44:00 PM**

Font: 10 pt, Font color: Black, English (UK)

▲  
**Page 20: [125] Formatted**      **Tzu-Hsuan Tu**      **10/17/21 10:44:00 PM**

Font: 10 pt, Font color: Black, English (UK)

▲  
**Page 20: [126] Formatted**      **Tzu-Hsuan Tu**      **10/17/21 10:44:00 PM**

Font: 10 pt, Font color: Black, English (UK)

▲  
**Page 20: [126] Formatted**      **Tzu-Hsuan Tu**      **10/17/21 10:44:00 PM**

Font: 10 pt, Font color: Black, English (UK)

▲  
**Page 20: [126] Formatted**      **Tzu-Hsuan Tu**      **10/17/21 10:44:00 PM**

Font: 10 pt, Font color: Black, English (UK)

▲  
**Page 20: [126] Formatted**      **Tzu-Hsuan Tu**      **10/17/21 10:44:00 PM**

Font: 10 pt, Font color: Black, English (UK)

▲  
**Page 20: [126] Formatted**      **Tzu-Hsuan Tu**      **10/17/21 10:44:00 PM**

Font: 10 pt, Font color: Black, English (UK)

▲  
**Page 20: [127] Formatted**      **Tzu-Hsuan Tu**      **10/17/21 10:44:00 PM**

Font: 10 pt, Font color: Black, English (UK)

▲  
**Page 20: [127] Formatted**      **Tzu-Hsuan Tu**      **10/17/21 10:44:00 PM**

Font: 10 pt, Font color: Black, English (UK)

▲  
**Page 20: [127] Formatted**      **Tzu-Hsuan Tu**      **10/17/21 10:44:00 PM**

Font: 10 pt, Font color: Black, English (UK)

▲  
**Page 20: [127] Formatted**      **Tzu-Hsuan Tu**      **10/17/21 10:44:00 PM**

Font: 10 pt, Font color: Black, English (UK)

▲  
**Page 20: [127] Formatted**      **Tzu-Hsuan Tu**      **10/17/21 10:44:00 PM**

Font: 10 pt, Font color: Black, English (UK)

▲  
**Page 20: [127] Formatted**      **Tzu-Hsuan Tu**      **10/17/21 10:44:00 PM**

Font: 10 pt, Font color: Black, English (UK)

▲  
**Page 20: [127] Formatted**      **Tzu-Hsuan Tu**      **10/17/21 10:44:00 PM**

Font: 10 pt, Font color: Black, English (UK)

▲  
**Page 20: [127] Formatted**      **Tzu-Hsuan Tu**      **10/17/21 10:44:00 PM**

Font: 10 pt, Font color: Black, English (UK)

Font: 10 pt, Font color: Black, English (UK)

▲  
**Page 20: [127] Formatted**      **Tzu-Hsuan Tu**      **10/17/21 10:44:00 PM**

Font: 10 pt, Font color: Black, English (UK)

▲  
**Page 20: [127] Formatted**      **Tzu-Hsuan Tu**      **10/17/21 10:44:00 PM**

Font: 10 pt, Font color: Black, English (UK)

▲  
**Page 20: [127] Formatted**      **Tzu-Hsuan Tu**      **10/17/21 10:44:00 PM**

Font: 10 pt, Font color: Black, English (UK)

▲  
**Page 20: [127] Formatted**      **Tzu-Hsuan Tu**      **10/17/21 10:44:00 PM**

Font: 10 pt, Font color: Black, English (UK)

▲  
**Page 20: [127] Formatted**      **Tzu-Hsuan Tu**      **10/17/21 10:44:00 PM**

Font: 10 pt, Font color: Black, English (UK)

▲  
**Page 20: [127] Formatted**      **Tzu-Hsuan Tu**      **10/17/21 10:44:00 PM**

Font: 10 pt, Font color: Black, English (UK)

▲  
**Page 20: [127] Formatted**      **Tzu-Hsuan Tu**      **10/17/21 10:44:00 PM**

Font: 10 pt, Font color: Black, English (UK)

▲  
**Page 20: [127] Formatted**      **Tzu-Hsuan Tu**      **10/17/21 10:44:00 PM**

Font: 10 pt, Font color: Black, English (UK)

▲  
**Page 20: [127] Formatted**      **Tzu-Hsuan Tu**      **10/17/21 10:44:00 PM**

Font: 10 pt, Font color: Black, English (UK)

▲  
**Page 20: [127] Formatted**      **Tzu-Hsuan Tu**      **10/17/21 10:44:00 PM**

Font: 10 pt, Font color: Black, English (UK)

▲  
**Page 20: [127] Formatted**      **Tzu-Hsuan Tu**      **10/17/21 10:44:00 PM**

Font: 10 pt, Font color: Black, English (UK)

▲  
**Page 20: [127] Formatted**      **Tzu-Hsuan Tu**      **10/17/21 10:44:00 PM**

Font: 10 pt, Font color: Black, English (UK)

▲  
**Page 20: [127] Formatted**      **Tzu-Hsuan Tu**      **10/17/21 10:44:00 PM**

Font: 10 pt, Font color: Black, English (UK)

▲  
**Page 20: [127] Formatted**      **Tzu-Hsuan Tu**      **10/17/21 10:44:00 PM**

Font: 10 pt, Font color: Black, English (UK)

▲  
**Page 20: [127] Formatted**      **Tzu-Hsuan Tu**      **10/17/21 10:44:00 PM**

Font: 10 pt, Font color: Black, English (UK)

▲

**Page 20: [127] Formatted**      **Tzu-Hsuan Tu**      **10/17/21 10:44:00 PM**

Font: 10 pt, Font color: Black, English (UK)

**Page 20: [127] Formatted**      **Tzu-Hsuan Tu**      **10/17/21 10:44:00 PM**

Font: 10 pt, Font color: Black, English (UK)

**Page 20: [127] Formatted**      **Tzu-Hsuan Tu**      **10/17/21 10:44:00 PM**

Font: 10 pt, Font color: Black, English (UK)

**Page 20: [127] Formatted**      **Tzu-Hsuan Tu**      **10/17/21 10:44:00 PM**

Font: 10 pt, Font color: Black, English (UK)

**Page 20: [127] Formatted**      **Tzu-Hsuan Tu**      **10/17/21 10:44:00 PM**

Font: 10 pt, Font color: Black, English (UK)

**Page 20: [127] Formatted**      **Tzu-Hsuan Tu**      **10/17/21 10:44:00 PM**

Font: 10 pt, Font color: Black, English (UK)

**Page 20: [127] Formatted**      **Tzu-Hsuan Tu**      **10/17/21 10:44:00 PM**

Font: 10 pt, Font color: Black, English (UK)

**Page 20: [127] Formatted**      **Tzu-Hsuan Tu**      **10/17/21 10:44:00 PM**

Font: 10 pt, Font color: Black, English (UK)

**Page 20: [127] Formatted**      **Tzu-Hsuan Tu**      **10/17/21 10:44:00 PM**

Font: 10 pt, Font color: Black, English (UK)

**Page 20: [127] Formatted**      **Tzu-Hsuan Tu**      **10/17/21 10:44:00 PM**

Font: 10 pt, Font color: Black, English (UK)

**Page 20: [127] Formatted**      **Tzu-Hsuan Tu**      **10/17/21 10:44:00 PM**

Font: 10 pt, Font color: Black, English (UK)

**Page 20: [128] Formatted**      **Tzu-Hsuan Tu**      **10/17/21 10:44:00 PM**

Font: 10 pt, Font color: Black, English (UK)

**Page 20: [129] Formatted**      **Tzu-Hsuan Tu**      **10/17/21 10:44:00 PM**

Font: 10 pt, Font color: Black, English (UK)

**Page 20: [129] Formatted**      **Tzu-Hsuan Tu**      **10/17/21 10:44:00 PM**

Font: 10 pt, Font color: Black, English (UK)

**Page 20: [129] Formatted**      **Tzu-Hsuan Tu**      **10/17/21 10:44:00 PM**

Font: 10 pt, Font color: Black, English (UK)

**Page 20: [129] Formatted**      **Tzu-Hsuan Tu**      **10/17/21 10:44:00 PM**

Font: 10 pt, Font color: Black, English (UK)

▲  
**Page 20: [130] Formatted**      **Tzu-Hsuan Tu**      **10/17/21 10:44:00 PM**

Font: 10 pt, Font color: Black, English (UK)

▲  
**Page 20: [131] Formatted**      **Tzu-Hsuan Tu**      **10/17/21 10:44:00 PM**

Font: 10 pt, Font color: Black, English (UK)

▲  
**Page 20: [132] Formatted**      **Tzu-Hsuan Tu**      **10/17/21 10:44:00 PM**

Font: 10 pt, Font color: Black, English (UK)

▲  
**Page 20: [133] Formatted**      **Tzu-Hsuan Tu**      **10/17/21 10:44:00 PM**

Font: 10 pt, Font color: Black, English (UK)

▲  
**Page 20: [133] Formatted**      **Tzu-Hsuan Tu**      **10/17/21 10:44:00 PM**

Font: 10 pt, Font color: Black, English (UK)

▲  
**Page 20: [134] Formatted**      **Tzu-Hsuan Tu**      **10/17/21 10:44:00 PM**

Font: 10 pt, Font color: Black, English (UK)

▲  
**Page 20: [135] Formatted**      **Tzu-Hsuan Tu**      **10/17/21 10:44:00 PM**

Font: 10 pt, Font color: Black, English (UK)

▲  
**Page 20: [135] Formatted**      **Tzu-Hsuan Tu**      **10/17/21 10:44:00 PM**

Font: 10 pt, Font color: Black, English (UK)

▲  
**Page 20: [136] Formatted**      **Tzu-Hsuan Tu**      **10/17/21 10:44:00 PM**

Font: 10 pt, Font color: Black

▲  
**Page 20: [136] Formatted**      **Tzu-Hsuan Tu**      **10/17/21 10:44:00 PM**

Font: 10 pt, Font color: Black

▲  
**Page 20: [137] Formatted**      **Tzu-Hsuan Tu**      **10/17/21 10:44:00 PM**

csl-entry

▲  
**Page 20: [138] Formatted**      **Tzu-Hsuan Tu**      **10/17/21 10:44:00 PM**

Font: 10 pt, Font color: Black, English (UK)

▲  
**Page 20: [139] Formatted**      **Tzu-Hsuan Tu**      **10/17/21 10:44:00 PM**

Font: 10 pt, Font color: Black, English (UK)

▲  
**Page 20: [140] Formatted**      **Tzu-Hsuan Tu**      **10/17/21 10:44:00 PM**

Font: 10 pt, Font color: Black, English (UK)

▲  
**Page 20: [141] Formatted**      **Tzu-Hsuan Tu**      **10/17/21 10:44:00 PM**

Font: 10 pt, Font color: Black, English (UK)

▲  
**Page 20: [141] Formatted**      **Tzu-Hsuan Tu**      **10/17/21 10:44:00 PM**

Font: 10 pt, Font color: Black, English (UK)

Font: 10 pt, Font color: Black, English (UK)

▲  
**Page 20: [141] Formatted**      **Tzu-Hsuan Tu**      **10/17/21 10:44:00 PM**

Font: 10 pt, Font color: Black, English (UK)

▲  
**Page 20: [141] Formatted**      **Tzu-Hsuan Tu**      **10/17/21 10:44:00 PM**

Font: 10 pt, Font color: Black, English (UK)

▲  
**Page 20: [142] Formatted**      **Tzu-Hsuan Tu**      **10/17/21 10:44:00 PM**

Font: 10 pt, Font color: Black, English (UK)

▲  
**Page 20: [142] Formatted**      **Tzu-Hsuan Tu**      **10/17/21 10:44:00 PM**

Font: 10 pt, Font color: Black, English (UK)

▲  
**Page 20: [142] Formatted**      **Tzu-Hsuan Tu**      **10/17/21 10:44:00 PM**

Font: 10 pt, Font color: Black, English (UK)

▲  
**Page 20: [142] Formatted**      **Tzu-Hsuan Tu**      **10/17/21 10:44:00 PM**

Font: 10 pt, Font color: Black, English (UK)

▲  
**Page 20: [143] Formatted**      **Tzu-Hsuan Tu**      **10/17/21 10:44:00 PM**

Font: 10 pt, Font color: Black, English (UK)

▲  
**Page 20: [144] Formatted**      **Tzu-Hsuan Tu**      **10/17/21 10:44:00 PM**

Font: 10 pt, Font color: Black, English (UK)

▲  
**Page 20: [144] Formatted**      **Tzu-Hsuan Tu**      **10/17/21 10:44:00 PM**

Font: 10 pt, Font color: Black, English (UK)

▲  
**Page 20: [144] Formatted**      **Tzu-Hsuan Tu**      **10/17/21 10:44:00 PM**

Font: 10 pt, Font color: Black, English (UK)

▲  
**Page 20: [144] Formatted**      **Tzu-Hsuan Tu**      **10/17/21 10:44:00 PM**

Font: 10 pt, Font color: Black, English (UK)

▲  
**Page 20: [145] Formatted**      **Tzu-Hsuan Tu**      **10/17/21 10:44:00 PM**

Font: 10 pt, Font color: Black, English (UK)

▲  
**Page 20: [145] Formatted**      **Tzu-Hsuan Tu**      **10/17/21 10:44:00 PM**

Font: 10 pt, Font color: Black, English (UK)

▲  
**Page 20: [145] Formatted**      **Tzu-Hsuan Tu**      **10/17/21 10:44:00 PM**

Font: 10 pt, Font color: Black, English (UK)

▲  
**Page 20: [145] Formatted**      **Tzu-Hsuan Tu**      **10/17/21 10:44:00 PM**

Font: 10 pt, Font color: Black, English (UK)

▲



**Page 20: [145] Formatted** Tzu-Hsuan Tu 10/17/21 10:44:00 PM

Font: 10 pt, Font color: Black, English (UK)

**Page 20: [145] Formatted** Tzu-Hsuan Tu 10/17/21 10:44:00 PM

Font: 10 pt, Font color: Black, English (UK)

**Page 20: [145] Formatted** Tzu-Hsuan Tu 10/17/21 10:44:00 PM

Font: 10 pt, Font color: Black, English (UK)

**Page 20: [145] Formatted** Tzu-Hsuan Tu 10/17/21 10:44:00 PM

Font: 10 pt, Font color: Black, English (UK)

**Page 20: [145] Formatted** Tzu-Hsuan Tu 10/17/21 10:44:00 PM

Font: 10 pt, Font color: Black, English (UK)

**Page 20: [146] Formatted** Tzu-Hsuan Tu 10/17/21 10:44:00 PM

Font: 10 pt, Font color: Black, English (UK)

**Page 20: [147] Formatted** Tzu-Hsuan Tu 10/17/21 10:44:00 PM

Font: 10 pt, Font color: Black, English (UK)

**Page 20: [148] Deleted** Tzu-Hsuan Tu 10/17/21 10:44:00 PM

**Page 20: [149] Formatted** Tzu-Hsuan Tu 10/17/21 10:44:00 PM

Font: 10 pt, Font color: Black, English (UK)

**Page 20: [150] Deleted** Tzu-Hsuan Tu 10/17/21 10:44:00 PM

**Page 20: [151] Formatted** Tzu-Hsuan Tu 10/17/21 10:44:00 PM

Font: 10 pt, Font color: Black, English (UK)

**Page 20: [151] Formatted** Tzu-Hsuan Tu 10/17/21 10:44:00 PM

Font: 10 pt, Font color: Black, English (UK)

**Page 20: [152] Formatted** Tzu-Hsuan Tu 10/17/21 10:44:00 PM

Font: 10 pt, Font color: Black, English (UK)

**Page 20: [153] Formatted** Tzu-Hsuan Tu 10/17/21 10:44:00 PM

Font: 10 pt, Font color: Black, English (UK)

**Page 20: [154] Formatted** Tzu-Hsuan Tu 10/17/21 10:44:00 PM

Font: 10 pt, Font color: Black, English (UK)

**Page 20: [154] Formatted** Tzu-Hsuan Tu 10/17/21 10:44:00 PM

**Page 20: [155] Formatted** Tzu-Hsuan Tu 10/17/21 10:44:00 PM

Font: 10 pt, Font color: Black, English (UK)

**Page 20: [156] Deleted** Tzu-Hsuan Tu 10/17/21 10:44:00 PM

**Page 20: [157] Formatted** Tzu-Hsuan Tu 10/17/21 10:44:00 PM

Font: 10 pt, Font color: Black, English (UK)

**Page 20: [158] Formatted** Tzu-Hsuan Tu 10/17/21 10:44:00 PM

Font: 10 pt, Font color: Black, English (UK)

**Page 20: [158] Formatted** Tzu-Hsuan Tu 10/17/21 10:44:00 PM

Font: 10 pt, Font color: Black, English (UK)

**Page 20: [158] Formatted** Tzu-Hsuan Tu 10/17/21 10:44:00 PM

Font: 10 pt, Font color: Black, English (UK)

**Page 20: [159] Formatted** Tzu-Hsuan Tu 10/17/21 10:44:00 PM

Font: 10 pt, Font color: Black, English (UK)

**Page 20: [160] Formatted** Tzu-Hsuan Tu 10/17/21 10:44:00 PM

Font: 10 pt, Font color: Black, English (UK)

**Page 20: [161] Formatted** Tzu-Hsuan Tu 10/17/21 10:44:00 PM

Font: 10 pt, Font color: Black, English (UK)

**Page 20: [162] Formatted** Tzu-Hsuan Tu 10/17/21 10:44:00 PM

Font: 10 pt, Font color: Black, English (UK)

**Page 20: [163] Formatted** Tzu-Hsuan Tu 10/17/21 10:44:00 PM

Font: 10 pt, Font color: Black, English (UK)

**Page 20: [164] Formatted** Tzu-Hsuan Tu 10/17/21 10:44:00 PM

Font: 10 pt, Font color: Black, English (UK)

**Page 20: [165] Formatted** Tzu-Hsuan Tu 10/17/21 10:44:00 PM

csl-entry

**Page 20: [166] Formatted** Tzu-Hsuan Tu 10/17/21 10:44:00 PM

Font: 10 pt, Font color: Black, English (UK)

**Page 20: [166] Formatted** Tzu-Hsuan Tu 10/17/21 10:44:00 PM

Font: 10 pt, Font color: Black, English (UK)

▲  
**Page 20: [166] Formatted**      **Tzu-Hsuan Tu**      **10/17/21 10:44:00 PM**

Font: 10 pt, Font color: Black, English (UK)

▲  
**Page 20: [166] Formatted**      **Tzu-Hsuan Tu**      **10/17/21 10:44:00 PM**

Font: 10 pt, Font color: Black, English (UK)

▲  
**Page 20: [166] Formatted**      **Tzu-Hsuan Tu**      **10/17/21 10:44:00 PM**

Font: 10 pt, Font color: Black, English (UK)

▲  
**Page 20: [167] Formatted**      **Tzu-Hsuan Tu**      **10/17/21 10:44:00 PM**

Font: 10 pt, Font color: Black, English (UK)

▲  
**Page 20: [167] Formatted**      **Tzu-Hsuan Tu**      **10/17/21 10:44:00 PM**

Font: 10 pt, Font color: Black, English (UK)

▲  
**Page 20: [167] Formatted**      **Tzu-Hsuan Tu**      **10/17/21 10:44:00 PM**

Font: 10 pt, Font color: Black, English (UK)

▲  
**Page 20: [168] Formatted**      **Tzu-Hsuan Tu**      **10/17/21 10:44:00 PM**

Font: 10 pt, Font color: Black, English (UK)

▲  
**Page 20: [169] Formatted**      **Tzu-Hsuan Tu**      **10/17/21 10:44:00 PM**

Font: 10 pt, Font color: Black, English (UK)

▲  
**Page 20: [170] Formatted**      **Tzu-Hsuan Tu**      **10/17/21 10:44:00 PM**

Font: 10 pt, Font color: Black, English (UK)

▲  
**Page 20: [170] Formatted**      **Tzu-Hsuan Tu**      **10/17/21 10:44:00 PM**

Font: 10 pt, Font color: Black, English (UK)

▲  
**Page 20: [170] Formatted**      **Tzu-Hsuan Tu**      **10/17/21 10:44:00 PM**

Font: 10 pt, Font color: Black, English (UK)

▲  
**Page 20: [171] Formatted**      **Tzu-Hsuan Tu**      **10/17/21 10:44:00 PM**

Font: 10 pt, Font color: Black, English (UK)

▲  
**Page 20: [172] Formatted**      **Tzu-Hsuan Tu**      **10/17/21 10:44:00 PM**

Font: 10 pt, Font color: Black, English (UK)

▲  
**Page 20: [172] Formatted**      **Tzu-Hsuan Tu**      **10/17/21 10:44:00 PM**

Font: 10 pt, Font color: Black, English (UK)

▲  
**Page 20: [173] Formatted**      **Tzu-Hsuan Tu**      **10/17/21 10:44:00 PM**

Font: 10 pt, Font color: Black, English (UK)

▲  
**Page 20: [174] Formatted**      **Tzu-Hsuan Tu**      **10/17/21 10:44:00 PM**

Font: 10 pt, Font color: Black, English (UK)

Font: 10 pt, Font color: Black, English (UK)

▲  
**Page 20: [174] Formatted**      **Tzu-Hsuan Tu**      **10/17/21 10:44:00 PM**

Font: 10 pt, Font color: Black, English (UK)

▲  
**Page 20: [175] Formatted**      **Tzu-Hsuan Tu**      **10/17/21 10:44:00 PM**

Font: 10 pt, Font color: Black, English (UK)

▲  
**Page 20: [176] Formatted**      **Tzu-Hsuan Tu**      **10/17/21 10:44:00 PM**

Font: 10 pt, Font color: Black, English (UK)

▲  
**Page 20: [176] Formatted**      **Tzu-Hsuan Tu**      **10/17/21 10:44:00 PM**

Font: 10 pt, Font color: Black, English (UK)

▲  
**Page 20: [177] Formatted**      **Tzu-Hsuan Tu**      **10/17/21 10:44:00 PM**

Font: 10 pt, Font color: Black, English (UK)

▲  
**Page 21: [178] Formatted**      **Tzu-Hsuan Tu**      **10/17/21 10:44:00 PM**

Font: 10 pt, Font color: Black, English (UK)

▲  
**Page 21: [178] Formatted**      **Tzu-Hsuan Tu**      **10/17/21 10:44:00 PM**

Font: 10 pt, Font color: Black, English (UK)

▲  
**Page 21: [178] Formatted**      **Tzu-Hsuan Tu**      **10/17/21 10:44:00 PM**

Font: 10 pt, Font color: Black, English (UK)

▲  
**Page 21: [179] Formatted**      **Tzu-Hsuan Tu**      **10/17/21 10:44:00 PM**

Font: 10 pt, Font color: Black, English (UK)

▲  
**Page 21: [179] Formatted**      **Tzu-Hsuan Tu**      **10/17/21 10:44:00 PM**

Font: 10 pt, Font color: Black, English (UK)

▲  
**Page 21: [179] Formatted**      **Tzu-Hsuan Tu**      **10/17/21 10:44:00 PM**

Font: 10 pt, Font color: Black, English (UK)

▲  
**Page 21: [180] Formatted**      **Tzu-Hsuan Tu**      **10/17/21 10:44:00 PM**

Font: 10 pt, Font color: Black, English (UK)

▲  
**Page 21: [180] Formatted**      **Tzu-Hsuan Tu**      **10/17/21 10:44:00 PM**

Font: 10 pt, Font color: Black, English (UK)

▲  
**Page 21: [181] Formatted**      **Tzu-Hsuan Tu**      **10/17/21 10:44:00 PM**

Font: 10 pt, Font color: Black, English (UK)

▲  
**Page 21: [182] Formatted**      **Tzu-Hsuan Tu**      **10/17/21 10:44:00 PM**

Font: 10 pt, Font color: Black, English (UK)

▲

**Page 21: [182] Formatted**      **Tzu-Hsuan Tu**      **10/17/21 10:44:00 PM**

Font: 10 pt, Font color: Black, English (UK)

**Page 21: [182] Formatted**      **Tzu-Hsuan Tu**      **10/17/21 10:44:00 PM**

Font: 10 pt, Font color: Black, English (UK)

**Page 21: [183] Formatted**      **Tzu-Hsuan Tu**      **10/17/21 10:44:00 PM**

Font: 10 pt, Font color: Black, English (UK)

**Page 21: [184] Formatted**      **Tzu-Hsuan Tu**      **10/17/21 10:44:00 PM**

Font: 10 pt, Font color: Black, English (UK)

**Page 21: [185] Formatted**      **Tzu-Hsuan Tu**      **10/17/21 10:44:00 PM**

Font: 10 pt, Font color: Black, English (UK)

**Page 21: [186] Formatted**      **Tzu-Hsuan Tu**      **10/17/21 10:44:00 PM**

Font: 10 pt, Font color: Black, English (UK)

**Page 21: [187] Formatted**      **Tzu-Hsuan Tu**      **10/17/21 10:44:00 PM**

Font: 10 pt, Font color: Black

**Page 21: [187] Formatted**      **Tzu-Hsuan Tu**      **10/17/21 10:44:00 PM**

Font: 10 pt, Font color: Black

**Page 21: [188] Formatted**      **Tzu-Hsuan Tu**      **10/17/21 10:44:00 PM**

Font: 10 pt, Font color: Black, English (UK)

**Page 21: [188] Formatted**      **Tzu-Hsuan Tu**      **10/17/21 10:44:00 PM**

Font: 10 pt, Font color: Black, English (UK)

**Page 21: [189] Formatted**      **Tzu-Hsuan Tu**      **10/17/21 10:44:00 PM**

Font: 10 pt, Font color: Black, English (UK)

**Page 21: [190] Formatted**      **Tzu-Hsuan Tu**      **10/17/21 10:44:00 PM**

Font: 10 pt, Font color: Black, English (UK)

**Page 21: [190] Formatted**      **Tzu-Hsuan Tu**      **10/17/21 10:44:00 PM**

Font: 10 pt, Font color: Black, English (UK)

**Page 21: [191] Formatted**      **Tzu-Hsuan Tu**      **10/17/21 10:44:00 PM**

Font: 10 pt, Font color: Black, English (UK)

**Page 21: [192] Formatted**      **Tzu-Hsuan Tu**      **10/17/21 10:44:00 PM**

Font: 10 pt, Font color: Black, English (UK)

**Page 21: [193] Formatted**      **Tzu-Hsuan Tu**      **10/17/21 10:44:00 PM**

Font: 10 pt, Font color: Black, English (UK)

▲ **Page 21: [195] Formatted** Tzu-Hsuan Tu 10/17/21 10:44:00 PM

Font: 10 pt, Font color: Black, English (UK)

▲ **Page 21: [196] Formatted** Tzu-Hsuan Tu 10/17/21 10:44:00 PM

Font: 10 pt, Font color: Black, English (UK)

▲ **Page 21: [197] Deleted** Tzu-Hsuan Tu 10/17/21 10:44:00 PM

▲ **Page 21: [198] Formatted** Tzu-Hsuan Tu 10/17/21 10:44:00 PM

Font: 10 pt, Font color: Black, English (UK)

▲ **Page 21: [199] Deleted** Tzu-Hsuan Tu 10/17/21 10:44:00 PM

▲ **Page 21: [200] Formatted** Tzu-Hsuan Tu 10/17/21 10:44:00 PM

Font: 10 pt, Font color: Black, English (UK)

▲ **Page 21: [200] Formatted** Tzu-Hsuan Tu 10/17/21 10:44:00 PM

Font: 10 pt, Font color: Black, English (UK)

▲ **Page 21: [201] Formatted** Tzu-Hsuan Tu 10/17/21 10:44:00 PM

Font: 10 pt, Font color: Black, English (UK)

▲ **Page 21: [202] Formatted** Tzu-Hsuan Tu 10/17/21 10:44:00 PM

Font: 10 pt, Font color: Black, English (UK)

▲ **Page 21: [203] Formatted** Tzu-Hsuan Tu 10/17/21 10:44:00 PM

Font: 10 pt, Font color: Black, English (UK)

▲ **Page 21: [204] Formatted** Tzu-Hsuan Tu 10/17/21 10:44:00 PM

Font: 10 pt, Font color: Black, English (UK)

▲ **Page 21: [205] Formatted** Tzu-Hsuan Tu 10/17/21 10:44:00 PM

csl-entry

▲ **Page 21: [206] Formatted** Tzu-Hsuan Tu 10/17/21 10:44:00 PM

Font: 10 pt, Font color: Black, English (UK)

▲ **Page 21: [206] Formatted** Tzu-Hsuan Tu 10/17/21 10:44:00 PM

Font: 10 pt, Font color: Black, English (UK)

▲  
**Page 21: [206] Formatted**      **Tzu-Hsuan Tu**      **10/17/21 10:44:00 PM**

Font: 10 pt, Font color: Black, English (UK)

▲  
**Page 21: [206] Formatted**      **Tzu-Hsuan Tu**      **10/17/21 10:44:00 PM**

Font: 10 pt, Font color: Black, English (UK)

▲  
**Page 21: [206] Formatted**      **Tzu-Hsuan Tu**      **10/17/21 10:44:00 PM**

Font: 10 pt, Font color: Black, English (UK)

▲  
**Page 21: [207] Formatted**      **Tzu-Hsuan Tu**      **10/17/21 10:44:00 PM**

Font: 10 pt, Font color: Black, English (UK)

▲  
**Page 21: [208] Formatted**      **Tzu-Hsuan Tu**      **10/17/21 10:44:00 PM**

Font: 10 pt, Font color: Black, English (UK)

▲  
**Page 21: [209] Formatted**      **Tzu-Hsuan Tu**      **10/17/21 10:44:00 PM**

Font: 10 pt, Font color: Black, English (UK)

▲  
**Page 21: [210] Formatted**      **Tzu-Hsuan Tu**      **10/17/21 10:44:00 PM**

Font: 10 pt, Font color: Black, English (UK)

▲  
**Page 21: [211] Formatted**      **Tzu-Hsuan Tu**      **10/17/21 10:44:00 PM**

Font: 10 pt, Font color: Black, English (UK)

▲  
**Page 21: [212] Formatted**      **Tzu-Hsuan Tu**      **10/17/21 10:44:00 PM**

Font: 10 pt, Font color: Black, English (UK)

▲  
**Page 21: [213] Formatted**      **Tzu-Hsuan Tu**      **10/17/21 10:44:00 PM**

Font: 10 pt, Font color: Black, English (UK)

▲  
**Page 21: [214] Formatted**      **Tzu-Hsuan Tu**      **10/17/21 10:44:00 PM**

Font: 10 pt, Font color: Black, English (UK)

▲  
**Page 21: [215] Formatted**      **Tzu-Hsuan Tu**      **10/17/21 10:44:00 PM**

Font: 10 pt, Font color: Black, English (UK)

▲  
**Page 21: [216] Formatted**      **Tzu-Hsuan Tu**      **10/17/21 10:44:00 PM**

Font: 10 pt, Font color: Black, English (UK)

▲  
**Page 21: [216] Formatted**      **Tzu-Hsuan Tu**      **10/17/21 10:44:00 PM**

Font: 10 pt, Font color: Black, English (UK)

▲  
**Page 21: [217] Formatted**      **Tzu-Hsuan Tu**      **10/17/21 10:44:00 PM**

Font: 10 pt, Font color: Black, English (UK)

▲  
**Page 21: [218] Formatted**      **Tzu-Hsuan Tu**      **10/17/21 10:44:00 PM**

Font: 10 pt, Font color: Black, English (UK)

Font: 10 pt, Font color: Black, English (UK)

▲  
**Page 21: [218] Formatted**      **Tzu-Hsuan Tu**      **10/17/21 10:44:00 PM**

Font: 10 pt, Font color: Black, English (UK)

▲  
**Page 21: [219] Formatted**      **Tzu-Hsuan Tu**      **10/17/21 10:44:00 PM**

Font: 10 pt, Font color: Black, English (UK)

▲  
**Page 21: [220] Formatted**      **Tzu-Hsuan Tu**      **10/17/21 10:44:00 PM**

Font: 10 pt, Font color: Black, English (UK)

▲  
**Page 21: [220] Formatted**      **Tzu-Hsuan Tu**      **10/17/21 10:44:00 PM**

Font: 10 pt, Font color: Black, English (UK)

▲  
**Page 21: [221] Formatted**      **Tzu-Hsuan Tu**      **10/17/21 10:44:00 PM**

Font: 10 pt, Font color: Black, English (UK)

▲  
**Page 21: [222] Formatted**      **Tzu-Hsuan Tu**      **10/17/21 10:44:00 PM**

Font: 10 pt, Font color: Black, English (UK)

▲  
**Page 21: [223] Formatted**      **Tzu-Hsuan Tu**      **10/17/21 10:44:00 PM**

Font: 10 pt, Font color: Black, English (UK)

▲  
**Page 21: [224] Formatted**      **Tzu-Hsuan Tu**      **10/17/21 10:44:00 PM**

Font: 10 pt, Font color: Black, English (UK)

▲  
**Page 21: [225] Formatted**      **Tzu-Hsuan Tu**      **10/17/21 10:44:00 PM**

Font: 10 pt, Font color: Black, English (UK)

▲  
**Page 21: [226] Formatted**      **Tzu-Hsuan Tu**      **10/17/21 10:44:00 PM**

Font: 10 pt, Font color: Black, English (UK)

▲  
**Page 21: [227] Formatted**      **Tzu-Hsuan Tu**      **10/17/21 10:44:00 PM**

English (US)

▲